Chapter 4

Feeder Load Balancing using Re-phasing of Loads

Phase-balancing creates voltage changes in the network which calls for incorporating voltage-dependency of loads in the process of phase-balancing. Hence, inclusion of voltage-dependency in current-injection based three-phase load flow is investigated and the results are compared with constant-power load model in terms of phase-balancing. The problem being combinatorial, application of particle swarm optimization is investigated for phase-balancing problem of radial distribution network. The effects of phase unbalance and load representation are studied in terms of various parameters. It is observed that there are situations that lead to increase in losses despite improvement in phase-balancing.

4.1 Introduction

The main substation transformers are one of the costliest devices in the distribution system. The MVA capacity is divided equally on three phases hence, the per-phase capacity is one-third of the MVA capacity of the transformer. As the time progresses the system load grows, however usually the load growth may not be equal on three phases. When the system loads are severely unbalanced, then if any of the phases gets loaded up to its capacity, the further loading of the main transformer gets restricted even when there may be sufficient capacity available

on other two phases. This may lead to load shedding on the loaded phase. Thus, in any system the load shedding limit would always be less than the total MVA capacity of the transformer. The re-phasing of loads tries to balance the currents of three phases so that the MVA capacity of the main transformer can be utilized fully and the load shedding limit gets extended. The phase unbalance in a system can create large voltage differences among the phases at a bus. The unbalanced phase voltages lead to unbalanced currents in three-phase loads at the customer site. This further restricts the transformer capacity at the customer site. Also, the unbalanced three phase load means higher negative- and zero-sequence current leading to losses for consumers which is not due to consumer. Also, in several cases the severe unbalance may not allow the consumer to use the machinery effectively. The unbalance in the system creates negative- and zero-sequence currents to flow in the system. The neutral conductor in the system is designed to carry small current compared to other phases assuming that the phases are balanced. The increased unbalance may ask for increased rating of neutral conductors. The neutral has a higher resistance compared to other phases and therefore, increase in neutral current increases the neutral losses also.

The process of phase-balancing ensures distribution of loads on three-phases in such a way that a minimum negative- and zero-sequence currents flow in the distribution system. This makes neutral current to be lowest and thereby having minimum loss in neutral conductors. A methodology to provide statistical estimates of unbalance is presented in [7]. The phase identification system [59] is applied to underground distribution transformers to automate the identification and correction for automated mapping fault management (AM/FM) system in Taipower.

Phase-balancing can be performed by power electronic hardware by injecting the compensating real- and reactive-power components into the distribution system [60]. Incorporation of loop-power controllers in presence of photovoltaic generation is reported in [61]. The hardware employed has its losses and cost of implementation and it injects harmonics. It is also possible to interchange the load being fed from one phase and neutral to another phase and neutral through

a switch. The load interchange mechanism has less hardware requirements and makes use of natural unbalance of the network.

An optimal three-phase power flow approach proposed in [62] uses voltage control equipments and other system components for minimizing the system voltage unbalance. The paper [62] introduces optimal power flow using newton type current-injection method along with interior-point optimization concept. There are different criterion on basis of which the load may be interchanged from one phase to another. The criteria could be (i) to balance the system loads so that all phases draw equal current from the main substation utilizing the full capacity of the main transformer; (ii) to reduce the losses of the system by reducing the neutral current; (iii) to have minimum current in the neutral conductor; (iv) to have balanced three-phase voltages at all the system 3-phase buses; (v) to reduce the flow of negative- and zero-sequence currents to avoid maloperation of relays.

The phase-balancing problem is such that even for moderate system the re-phasing combinations [63] explode into a huge number. It is one of the problems for which search based methods such as Genetic Algorithms (GA) or Particle Swarm Optimization (PSO) are best suited. There are other methods based on heuristics; such as fuzzy logic based techniques for getting a better phase-balancing scheme [12]. An expert system could be suitable choice for a particular system but cannot be generalized [64]. GA-based approach has been proposed to solve phase-balancing problem along with other objectives in a weighted form. The major objectives include phase-balancing of the loads, phase voltage unbalance factor and average voltage drop, neutral current of the main transformer and the system losses [13]. The authors have also indicated that when compared with other heuristic methods of phase-balancing the GA performed better. The advantage of load-time characteristics of different load types in a distribution system can be taken for re-arranging the transformer phases for obtaining load balancing. Thus, by proper arrangement of compositions of load types, the maximum utilization of capacity rating of distribution transformer can be arrived at [65]. The authors presented two methods of phase re-arrangement for reducing unbalance factor and also showed that the system losses reduce.

With adoption of new technologies focused towards smart-grid operations there is a need for serious attempts towards implementing some of the useful functions such as phase-balancing in distribution systems. The implementation of automation and measurement technologies have given some interesting insights into characteristics of distribution system operation such as increase in system power consumption despite implementing loss reducing strategies such as capacitor placement [14], under voltage load shedding [15], and feeder phase-balancing in certain conditions [16]. These phenomena were observed through practically acquired measurements, whereas, most of the studies in literature showed otherwise [16]. It is evident that automation technologies adopted would be useful only if proper model are used in operational studies. One of the simulation assumptions which need a serious review is load (model) representation in system operation studies. There have been efforts towards determining load model parameters in literature [66] [67] suggesting that such model parameters can be employed in the studies to get useful results for operational planning. Therefore an analysis of implications of not using appropriate load models in operational studies must also be assessed.

An important point made by authors in [16] regarding the impacts of unbalance compensation on feeder losses was that it may lead to slight increase in feeder losses. The two major effects of unbalance compensation were found to be as follows

i Unbalance compensation usually leads to loss reduction. The reduction in certain case could be to the tune of 15%.

ii Elimination of unbalance components at the low voltage bus of substation causes a slight increase in feeder's losses.

The first case is obvious; due to reduction in line flows of zero-sequence and negative-sequence currents in the circuit, the losses attributed to them would reduce. However, the second case is not very clear and is one of the subjects of investigation in this paper. It is shown that (ii) can be explained if the voltage-dependency of loads were considered.

In the present work a particle swarm based load balancing is implemented. First of all the extent up to which a feeder phase-balancing can be achieved through re-phasing of loads is demonstrated. One of the important characteristics of practical load is its voltage-dependency. In previous re-phasing studies, voltage-dependencies have not been included even though it is invariably shown that the bus voltages improve significantly, and still the loads are forced to be constant (load) during simulations. This paper investigates the voltage-dependency aspect of load and attempts to come up with a possible answer to some of the phenomena which have been reported in literature from field studies which do not match with the theoretical estimates [16]. The current-injection based [17] load flow is modified for inclusion of voltage-dependency of loads. The paper also discusses the detailed outcomes of phase-balancing in terms of MVA intakes, losses, bus-voltages, main substation transformer loading margins, phase currents and sequence currents.

4.2 Problem Formulation

The problem is formulated in three parts. The first part discusses the mathematical implementation of a load-switch which can transfer a load from one phase to the other. The second part gives a mathematical description of the load model and its inclusion in the current-injection based three-phase distribution load flow. The third part finally gives implementation of particle swarm based optimization for re-phasing problem.

4.2.1 Three-phase load change-over at distribution transformers

The load switch change-over for a particular load bus k, can be describe by following matrix

$$S^k = \begin{pmatrix} s_{11}^k & s_{12}^k & s_{13}^k \\ s_{21}^k & s_{22}^k & s_{23}^k \\ s_{31}^k & s_{32}^k & s_{33}^k \end{pmatrix} \tag{4.1}$$

where, $s_{ij}^k \in (1,0)$, $\sum_{i=1}^{3} s_{ij} = 1$, $j \in \{1,2,3\}$, $i \in \{1,2,3\}$, so that the load, real and reactive respectively, at the particular bus k, can be written as,

$$\bar{p}_k + j\bar{q}_k = S^k(\bar{p}_{Dk} + j\bar{q}_{Dk}) \tag{4.2}$$

where, $\bar{p}_k + j\bar{q}_k = \begin{pmatrix} p_k^{a,sp} + jq_k^{a,sp} \\ p_k^{b,sp} + jq_k^{b,sp} \\ p_k^{c,sp} + jq_k^{c,sp} \end{pmatrix}$,

$$\bar{p}_{Dk} + j\bar{q}_{Dk} = \begin{pmatrix} p_{Dk}^1 + jq_{Dk}^1 \\ p_{Dk}^2 + jq_{Dk}^2 \\ p_{Dk}^3 + jq_{Dk}^3 \end{pmatrix}.$$

Where, $\bar{p}_{Dk} + j\bar{q}_{Dk}$ are set of three phase load demands at bus k and $\bar{p}_k + j\bar{q}_k$ are the specified phase load at bus k.

4.2.2 Inclusion of voltage dependency of loads in 3-phase distribution load flow

Exponential load model is a general load model and can be used for modeling the loads in scenarios where the load dependency is of higher degree. The composite loads are special case where the exponents can take the fixed values of 0, 1 and 2. A static load model that represents the power relationship to voltage as an exponential equation [68], usually in the following form:

$$P = P_0 \left(\frac{|V|}{|V_0|}\right)^{\alpha}; Q = Q_0 \left(\frac{|V|}{|V_0|}\right)^{\beta}; \tag{4.3}$$

Two or more terms with different exponents are sometimes included in each equation. The parameters of this model are the exponents, α and β , and the power factor of the load. By setting these exponents to 0, 1, or 2, the load can be represented by constant power, constant current, or constant impedance models, respectively. Other exponents can be used to represent the aggregate effect of

different types of load components. Exponents greater than 2 or less than 0 may be appropriate for some types of loads. A reason for having such values are given in [69] as follows. In case of exponential load model, it may be noted that in actual studies the α goes up to 1.8 whereas the β values corresponding to reactive power go up to 6. Therefore, if reactive load is modeled as ZIP model, it may not match the measured characteristics for reactive loads. The significant characteristic of reactive load is that it varies as a nonlinear function of voltage characterized by the high value of β. This is caused by magnetic saturation in distribution transformers and motors.

The power flow algorithm is based on approach followed in [17]. The modifications are made to the load flow algorithm to include the exponential load model. The voltage control equipments can be considered on the same lines as in [17] and [70].

In the load flow algorithm, the load specified at bus i and phase j during k^{th} iteration can be written as voltage-dependent load in the following way,

$$p_i^{j,sp,k} = p_{i0}^{j,sp,k} \left(\frac{|V_i^{j,k}|}{|V_{i0}|} \right)^{\alpha^j} ; q_i^{j,sp,k} = q_{i0}^{j,sp,k} \left(\frac{|V_i^{j,k}|}{|V_{i0}|} \right)^{\beta^j} \tag{4.4}$$

$j \in \{a, b, c\}$. A flat start for $|V_i^{j,k}|$'s are taken. Using the voltages $|V_i^{j,k}|$ the loads can be calculated as

$$p_i^{j,cal,k} - jq_i^{j,cal,k} = \bar{V}_i^{*j,k} . \sum_{j=1}^{N} \sum_{m \in a,b,c} Y_{i,j}^m . \bar{V}_j^{m,k} \tag{4.5}$$

The load flow converges if the tolerance value ϵ is less than a prescribed tolerance where,

$$\epsilon = \max_{i \in all\ load\ busses} \{ |p_i^{j,sp,k} - p_i^{j,cal,k}|, |q_i^{j,sp,k} - q_i^{j,cal,k}| \} \tag{4.6}$$

The specified equivalent loads ($P_i^{j,sp,k}$ and $Q_i^{j,sp,k}$) at bus i, phase j, at the k^{th} iteration can be obtained as sum of powers being supplied to all the buses downstream.

$$P_i^{j,sp,k} = \sum_l p_l^{j,sp,k} + \sum_{(p-q)} p_{L,(p-q)}^{j,k} \tag{4.7}$$

$$Q_i^{j,sp,k} = \sum_l q_l^{j,sp,k} + \sum_{(p-q)} q_{L,(p-q)}^{j,k} \tag{4.8}$$

where, $l \in$ *bus downstream of* i, and $(p-q) \in$ *lines downstream of* i. $p^{j,k}_{L,(p-q)}$, $q^{j,k}_{L,(p-q)}$, are the real and reactive losses in line $(p-q)$, for the j^{th} phase at the k^{th} iteration. The specified bus loads can be converted to Equivalent Current Injections (ECI) using the following relation.

$$\bar{I}_i^{j,ECI,k} = \frac{P_i^{j,sp,k} - jQ_i^{j,sp,k}}{\bar{V}_i^{*,j,k}} \tag{4.9}$$

where $\bar{I}_i^{j,ECI,k} = i_i^{r,j,ECI,k} + ji_i^{i,j,ECI,k}$, and $\bar{V}_i^{j,k} = e_i^{j,k} + jf_i^{j,k}$. The calculated three-phase currents for a particular feeder section $p-i$ can be given by the following expression.

$$\begin{pmatrix} \bar{I}_i^{a,cal,k} \\ \bar{I}_i^{b,cal,k} \\ \bar{I}_i^{c,cal,k} \end{pmatrix} = \begin{pmatrix} y_{p-i}^{aa} & y_{p-i}^{ab} & y_{p-i}^{ac} \\ y_{p-i}^{ba} & y_{p-i}^{bb} & y_{p-i}^{bc} \\ y_{p-i}^{ca} & y_{p-i}^{cb} & y_{p-i}^{cc} \end{pmatrix} \begin{pmatrix} \bar{V}_p^{a,k} - \bar{V}_i^{a,k} \\ \bar{V}_p^{b,k} - \bar{V}_i^{b,k} \\ \bar{V}_p^{c,k} - \bar{V}_i^{c,k} \end{pmatrix} \tag{4.10}$$

where, $y_{p-i}^{aa} = g_{p-i}^{aa} + jb_{p-i}^{aa}$, $\bar{I}_i^{a,cal,k} = i_i^{r,a,cal,k} + ji_i^{i,a,cal,k}$, or $\bar{I}_i^{a,cal,k} = y_{p-i}^{aa}(\bar{V}_p^{a,k} - \bar{V}_i^{a,k}) + y_{p-i}^{ab}(\bar{V}_p^{b,k} - \bar{V}_i^{b,k}) + y_{p-i}^{ac}(\bar{V}_p^{c,k} - \bar{V}_i^{c,k})$. From (4.10), the incremental relation between the currents injections and node voltages for phase a can be written as

$$\begin{pmatrix} \Delta i_i^{r,a,cal,k} \\ \Delta i_i^{i,a,cal,k} \end{pmatrix} = \begin{pmatrix} g_{p-i}^{aa} & -b_{p-i}^{aa} \\ b_{p-i}^{aa} & g_{p-i}^{aa} \end{pmatrix} \begin{pmatrix} \Delta e_i^{a,k} \\ \Delta f_i^{a,k} \end{pmatrix} \tag{4.11}$$

The above relationship for all the three-phases may be written as

$$\begin{pmatrix} \Delta i_i^{r,a,cal,k} \\ \Delta i_i^{i,a,cal,k} \\ \Delta i_i^{r,b,cal,k} \\ \Delta i_i^{i,b,cal,k} \\ \Delta i_i^{r,c,cal,k} \\ \Delta i_i^{i,c,cal,k} \end{pmatrix} = \Big[GB\Big] \begin{pmatrix} \Delta e_i^{a,k} \\ \Delta f_i^{a,k} \\ \Delta e_i^{b,k} \\ \Delta f_i^{b,k} \\ \Delta e_i^{c,k} \\ \Delta f_i^{c,k} \end{pmatrix} \tag{4.12}$$

where,

$$\Big[GB\Big] = \begin{pmatrix} g_{p-i}^{aa} & -b_{p-i}^{aa} & g_{p-i}^{ab} & -b_{p-i}^{ab} & g_{p-i}^{ac} & -b_{p-i}^{ac} \\ b_{p-i}^{aa} & g_{p-i}^{aa} & b_{p-i}^{ab} & g_{p-i}^{ab} & b_{p-i}^{ac} & g_{p-i}^{ac} \\ g_{p-i}^{ba} & -b_{p-i}^{ba} & g_{p-i}^{bb} & -b_{p-i}^{bb} & g_{p-i}^{bc} & -b_{p-i}^{bc} \\ b_{p-i}^{ba} & g_{p-i}^{ba} & b_{p-i}^{bb} & g_{p-i}^{bb} & b_{p-i}^{bc} & g_{p-i}^{bc} \\ g_{p-i}^{ca} & -b_{p-i}^{ca} & g_{p-i}^{cb} & -b_{p-i}^{cb} & g_{p-i}^{cc} & -b_{p-i}^{cc} \\ b_{p-i}^{ca} & g_{p-i}^{ca} & b_{p-i}^{cb} & g_{p-i}^{cb} & b_{p-i}^{cc} & g_{p-i}^{cc} \end{pmatrix}$$

The incremental feeder current for phase a can be calculated from (4.9) and (4.10) as follows.

$$\begin{pmatrix} \Delta i_i^{r,a,cal,k} \\ \Delta i_i^{i,a,cal,k} \end{pmatrix} = \begin{pmatrix} i_i^{r,a,ECI,k} \\ i_i^{i,a,ECI,k} \end{pmatrix} - \begin{pmatrix} i_i^{r,a,cal,k} \\ i_i^{i,a,cal,k} \end{pmatrix} \tag{4.13}$$

The solution for $[\ \Delta e_i^{a,k}\ \Delta f_i^{a,k}\ \Delta e_i^{b,k}\ \Delta f_i^{b,k}\ \Delta e_i^{c,k}\ \Delta f_i^{c,k}\ ]^T$ at k^{th} iteration is obtained by substituting the RHS of (4.13) in LHS of (4.12). Using this solution, the expression for phase voltages at bus i for $k+1^{th}$ iteration is obtained as follows.

$$\begin{pmatrix} e_i^{a,k+1} \\ f_i^{a,k+1} \\ e_i^{b,k+1} \\ f_i^{b,k+1} \\ e_i^{c,k+1} \\ f_i^{c,k+1} \end{pmatrix} = \begin{pmatrix} e_i^{a,k} \\ f_i^{a,k} \\ e_i^{b,k} \\ f_i^{b,k} \\ e_i^{c,k} \\ f_i^{c,k} \end{pmatrix} + \begin{pmatrix} \Delta e_i^{a,k} \\ \Delta f_i^{a,k} \\ \Delta e_i^{b,k} \\ \Delta f_i^{b,k} \\ \Delta e_i^{c,k} \\ \Delta f_i^{c,k} \end{pmatrix} \tag{4.14}$$

The updated voltage values of (4.14) are used to compute the new values of bus powers using (4.4) and the procedure is repeated till the tolerance is met.

4.2.3 Particle Swarm based phase load balancing

The particle swarm optimization (PSO) is a parallel evolutionary computation technique developed by Kennedy and Eberhart [71] based on the social behavior metaphor. Reynolds [72] proposed a behavioral model in which each of the particles follows three rules for finding the food.

i Separation: Each particle tries to move away from its neighbors if they are too close.

ii Alignment: Each particle steers towards a general direction of neighbouring particles.

iii Cohesion: Each particle tries to go towards the general position of its neighbors.

The PSO algorithm is initialized with a population of random particles (candidate solution vectors). Each particle is characterized by its position (solution vector) and velocity (direction in which it will move toward a new solution vector in the problem space). For each particle a random velocity is assigned initially. Each particle iteratively moves in the problem space. Using above stated behavioral model the particle moves towards the position of minimum value of the objective function (or best fitness) achieved so far by the particle itself and towards the position of the best fitness achieved so far by the whole population. For following optimization problem, $\bar{x}^* \subseteq \bar{X} \subseteq \mathbb{R}^n$ such that $\bar{x}^* = \underset{\bar{x}\in\bar{X}}{arg\ min} f(\bar{x}) = \{\bar{x}^* \in \bar{X} : f(\bar{x}^*) \leq f(\bar{x})\}$, the PSO algorithm updates the velocity and position of particles in the following manner at k^{th} iteration.

$$\bar{v}^{k+1} = m_v \bigotimes \bar{v}^k + m_{x1} \bigotimes \bar{r1} \bigotimes (\bar{p_1} - \bar{x}^k) + m_{x2} \bigotimes \bar{r_2} \bigotimes (\bar{p_2} - \bar{x}^k) \quad (4.15)$$

$$\bar{x}^{k+1} = c_x \bigotimes \bar{x}^k + c_v \bigotimes \bar{r1} \bigotimes \bar{v}^{k+1} \quad (4.16)$$

The symbol $\bigotimes$ denotes element-by-element vector multiplication. m_v, m_{x1}, and m_{x2} are momentum values, $\bar{r}_1$ and $\bar{r}_2$ are the random vectors. $\bar{p}_1$ is called local-best solution, a solution vector having best fit achieved so far (up to the k^{th} iteration) by the particular particle $\bar{x}^k$ and $\bar{p}_2$ is called the global solution. It is a solution vector having best fit achieved so far by among the swarm (up to the k^{th} iteration). The new solution vector $\bar{x}^{k+1}$ is obtained by linearly combining the last position $\bar{x}^k$ and velocity $\bar{v}^{k+1}$. In the present work particle swarm algorithm has been applied to get the optimal or sub-optimal solution for feeder phase-balancing. The objective is to redistribute the loads at each of the buses among the three-phases resulting in minimum negative- and zero- sequence currents. The current unbalance index using the complementary unbalance definition [**?**] considering the zero-sequence components as well as the negative-sequence components have been used. The optimization problem for feeder re-phasing for minimum unbalance index, Root Mean Squared Current ($RMSI$), can be stated as follows. Determine the matrix vectors $S=([S^1],[S^2],...,[S^n])$ on all the buses $i = 1, 2, 3, ...n$ which minimizes

$$RMSI(S) = \frac{\sqrt{(|I_0(S)|^2 + |I_2(S)|^2)}}{|I_1(S)|} \quad (4.17)$$

such that the following constraints are satisfied.

$$\begin{aligned} p_i^j(S) = e_i^j(S) \sum_{k=1}^{n} \sum_{m} (G_{ik}^{j,m} e_k^m(S) + B_{ik}^{j,m} f_k^m(S)) \\ + f_i^j(S) \sum_{k=1}^{n} \sum_{m} (G_{ik}^{j,m} f_k^m(S) - B_{ik}^{j,m} e_k^m(S)) \end{aligned} \tag{4.18}$$

$$\begin{aligned} q_i^j(S) = f_i^j(S) \sum_{k=1}^{n} \sum_{m} (G_{ik}^{j,m} e_k^m(S) + B_{ik}^{j,m} f_k^m(S)) \\ - e_i^j(S) \sum_{k=1}^{n} \sum_{m} (G_{ik}^{j,m} f_k^m(S) - B_{ik}^{j,m} e_k^m(S)); \end{aligned} \tag{4.19}$$

$m \in \{a,b,c\}$

$$p_i^j(S) = p_{i0}^j(S) \left(\frac{|V_i^j(S)|}{|V_{i0}|} \right)^{\alpha^{j(S)}} \tag{4.20}$$

$$q_i^j(S) = q_{i0}^j(S) \left(\frac{|V_i^j(S)|}{|V_{i0}|} \right)^{\beta^{j(S)}} \tag{4.21}$$

Considering node#1 as root node or main sub-station node the sequence currents at the main sub-station are as follows.

$$\begin{pmatrix} I_1(S) \\ I_2(S) \\ I_0(S) \end{pmatrix} = \frac{1}{3} \begin{pmatrix} 1 & \alpha & \alpha^2 \\ 1 & \alpha^2 & \alpha \\ 1 & 1 & 1 \end{pmatrix} \begin{pmatrix} y_{1-2}^{aa} & y_{1-2}^{ab} & y_{1-2}^{ac} \\ y_{1-2}^{ba} & y_{1-2}^{bb} & y_{1-2}^{bc} \\ y_{1-2}^{ca} & y_{1-2}^{cb} & y_{1-2}^{cc} \end{pmatrix} \begin{pmatrix} \bar{V}_1^a(S) - \bar{V}_2^a(S) \\ \bar{V}_1^b(S) - \bar{V}_2^b(S) \\ \bar{V}_1^c(S) - \bar{V}_2^c(S) \end{pmatrix} \tag{4.22}$$

The flow-chart showing the phase balancing proceedure using PSO is shown in Figure 4.1. Each particle 'Si' corresponds to a set of 25 (number of buses) elements and each element is an integer code taking values from 1 to 6. Each integer code corresponds to one of the six possible switching matrices. A particle x˙k at k˙th iterarion will have 25 elements as explained below for a sample particle.
$\bar{x}^k = Si = [6, 3, 5, 2, 3, 1, 4, 2, 6, 3, 5, 2, 3, 5, 2, 2, 4, 1, 6, 3, 2, 5, 1, 3, 6]$
The $RMSI(Si)$ is used as a fitness function for a particle Si. The velocities and positions for the particles are updated according to equations (4.15), and (4.16). The algorithm was assumed to converge, when for the last thousand iterations there is no change in fitness and difference in position is less than 0.0001.

Table 4.1: Impedance Matices for the conductor types (in ohm/mile)

Type			
#1	0.3686 + 0.6852i	0.0169 + 0.1515i	0.0155 + 0.1098i
	0.0169 + 0.1515i	0.3757 + 0.6715i	0.0188 + 0.2072i
	0.0155 + 0.1098i	0.0188 + 0.2072i	0.3723 + 0.6782i
#2	0.9775 + 0.8717i	0.0167 + 0.1697i	0.0152 + 0.1264i
	0.0167 + 0.1697i	0.9844 + 0.8654i	0.0186 + 0.2275i
	0.0152 + 0.1264i	0.0186 + 0.2275i	0.9810 + 0.8648i
#3	1.9280 + 1.4194i	0.0161 + 0.1183i	0.0161 + 0.1183i
	0.0161 + 0.1183i	1.9308 + 1.4215i	0.0161 + 0.1183i
	0.0161 + 0.1183i	0.0161 + 0.1183i	1.9337 + 1.4236i

4.3 Test System and Studies performed

The single line diagram, showing line type and line length (ft.), of a 25-bus, 3-phase, test system [73] shown in Figure 5.1, has been used for studying the re-phasing scheme proposed in this chapter. The base load data of this system and the voltage exponents for active power, α^j, and reactive power, β^j, $j \in \{a, b, c\}$ for each bus, are given in Table 4.2. The slack bus voltage is taken as 1.05 p.u. The nominal voltage $|V_{i0}|$ is taken as 1.0 $p.u.$. The sample values of the exponents are adopted from [68]. The impedance matrices for the conductor types [73] are given in Table 4.1 . The current injection based three-phase load flow algorithm given in section 5.2.2 is used for load flow analysis. When the load data is assumed to be of constant load type, the real and reactive power exponents are set to 0. The calculations were made on bases of $100kVA$ and $2.4kV$.

The parameters of PSO algorithm used are as follows: $m_v = m_{x1} = m_{x2} = 1$, $c_x = 0.01$, and $c_v = 0.02$. A particle consists of 25 elements, and each element is an integer code taking values from 1 to 6. Each integer code corresponds to one of the six possible switching matrices. The algorithm takes the integer code and converts it into a corresponding switching matrix and then transforms it into an equivalent three-phase load. Corresponding to these equivalent loads the fitness

Table 4.2: Specified real and reactive power and voltage exponents for the test system

Bus #	p_{i0}^a jq_{i0}^a	$p_{i0}^b jq_{i0}^b$	$p_{i0}^c jq_{i0}^c$	α^a β^a	α^b β^b	α^c β^c
1	00.0 00.0	00.0 00.0	00.0 00.0	0.00 0.00	0.00 0.00	0.00 0.00
2	00.0 00.0	00.0 00.0	00.0 00.0	0.00 0.00	0.00 0.00	0.00 0.00
3	36.0 21.6	28.8 19.2	42.0 26.4	0.92 4.04	0.18 4.04	0.18 6.00
4	57.6 43.2	04.8 03.4	48.0 30.0	0.18 6.00	0.92 4.04	0.18 6.00
5	43.2 28.8	28.8 19.2	36.0 24.0	1.51 3.40	1.51 3.40	1.51 3.40
6	43.2 28.8	33.6 24.0	30.0 30.0	1.51 3.40	0.18 6.00	0.92 4.04
7	00.0 00.0	00.0 00.0	00.0 00.0	0.00 0.00	0.00 0.00	0.00 0.00
8	43.2 28.8	28.8 19.2	03.6 02.4	1.51 3.40	1.51 3.40	0.92 4.04
9	72.0 50.4	38.4 28.8	48.0 30.0	0.18 6.00	0.18 6.00	0.18 6.00
10	36.0 21.6	28.8 19.2	42.0 26.4	0.92 4.04	1.51 4.04	0.18 6.00
11	50.4 31.7	24.0 14.4	36.0 24.0	0.18 6.00	0.92 4.04	1.51 3.40
12	57.6 36.0	48.0 33.6	48.0 36.0	0.18 6.00	0.18 6.00	0.18 6.00
13	64.8 21.6	33.6 21.1	36.0 24.0	0.92 4.04	0.18 6.00	1.51 3.40
14	57.6 36.0	38.4 28.8	60.0 42.0	0.18 6.00	0.18 6.00	0.18 6.00
15	07.2 04.3	04.8 02.9	06.0 03.6	0.92 4.04	0.18 6.00	0.18 6.00
16	57.6 04.3	03.8 28.8	48.0 36.0	1.51 3.40	0.92 4.04	1.51 3.40
17	57.6 43.2	33.6 24.0	54.0 38.4	1.51 3.40	0.92 4.04	0.18 6.00
18	57.6 43.2	38.4 28.8	48.0 36.0	1.51 3.40	1.51 3.40	1.51 3.40
19	08.6 06.5	04.8 03.4	06.0 04.8	0.18 6.00	1.51 3.40	0.18 6.00
20	50.4 36.0	38.4 28.8	54.0 38.4	0.92 4.04	1.51 3.40	1.51 3.40
21	05.8 04.3	03.4 02.4	05.4 03.8	1.51 3.40	0.92 4.04	1.51 3.40
22	72.0 50.4	57.6 43.2	60.0 48.0	0.18 6.00	1.51 3.40	0.18 6.00
23	08.6 64.8	04.8 03.8	60.0 42.0	0.92 4.04	0.92 4.04	0.18 6.00
24	50.4 36.0	43.2 30.7	04.8 03.6	0.92 4.04	1.51 3.40	0.92 4.04
25	08.6 06.5	04.8 02.9	06.0 04.2	0.92 4.04	1.51 3.40	0.18 6.00

function (RMSI) is calculated using the results obtained from the power flow. The stopping criteria used is quite stringent one i.e. the PSO is assumed to converge when for last 1000 iterations, (i) there is no change in $RMSI$, and (ii) $\|\bar{x}_k - \bar{x}_{k-1000}\|_1 \leq 0.0001$

The following case studies are performed in this work.

1. *Case* 1: In this case re-phasing is performed using constant load model to estimate the extent up to which the balancing can be achieved and its benefits can be derived when loads of distribution system are assumed to be constant.

2. *Case* 2: In this case re-phasing is performed using voltage-dependent load models to estimate the effect of voltage-dependency on phase balancing that can be achieved and benefits that can be derived compared to *Case* 1.

3. *Case* 3: In this case the re-phasing is obtained using constant load model i.e. of *Case*1. This re-phasing is applied to actual scenario of voltage-dependent loads. This post analysis is performed to estimate the effect of voltage dependency of loads of distribution system which is re-phased using constant load model.

4.4 Results and Discussions

The test system parameters for the base case loading and the parameters obtained after phase-wise redistribution of bus-loads (re-phasing) are shown in Table 4.3. The parameters for various scenarios are depicted in Table 4.3. These scenarios are as follows: (i) *Base-C* corresponds to base case for constant load model, (ii) *Re-phased-C* corresponds to the case where re-phasing is obtained using constant load model, (iii) *Base-V-D* corresponds to the base case for voltage-dependent load model, (iv) *Re-phased-V-D* corresponds to the case when the re-phasing is obtained using voltage-dependent load model, (v) *Re-phased-Error* corresponds to the case where re-phasing is obtained using constant load model subjected to actual scenario of voltage-dependent loads.The bus-load demands in case of voltage-dependent loads are found to be different from the constant bus-load model, since load at any bus is a function of voltage at that bus. In Table 4.3 the parameters considered for comparison are (i) per phase real demand and reactive demand at main sub-station (p_d^j, q_d^j), (ii) per phase MVA demands at main sub-station (s_d^j), (iii) amount of per phase MVA transfer (load off-loaded from/ load added to a particular phase) after re-phasing compared with base case (Δs_d^j), (iv) the actual per phase MVA intake at the main sub-station (s_a^j), (v) phase-wise MVA margins (s_{margin}^j) available at the main sub-station considering main substation transformer capacity of 1100 kVA (3300/3 kVA), and (vi) per phase real and reactive losses (p_{loss}^j, q_{loss}^j).

Table 4.3: Results of Re-phasing for different scenarios

Parameters	Phase a	Phase b	Phase c
$\mathbf{p_d^j}$(kW), $\mathbf{q_d^j}$(kvar)			
Base-C	946.08, 648	573.6, 430.56	781.8, 554.04
Re-phased-C	766.44, 546.24	763.2, 542.04	771.84, 544.32
Base-V-D	951.64, 666.21	586.93, 475.19	789.43, 594.74
Re-phased-V-D	778.99, 580.20	772.32, 585.94	778.64, 579.23
Re-phased-Error	775.16, 582.23	772.84, 582.23	782.11, 588.40
$\mathbf{s_d^j}$ (kVA)			
Base-C	1146.72	717.22	958.21
Re-phased-C	941.17	936.1	944.47
Base-V-D	1161.66	755.18	988.48
Re-phased-V-D	971.31	969.43	970.45
Re-phased-Error	969.47	967.62	978.73
$\mathbf{\Delta s_d^j}$ (kVA)			
Base-C	-	-	
Re-phased-C	206.46(off-loaded)	219.95(added)	13.92(off-loaded)
Base-V-D	-	-	-
Re-phased-V-D	192.89(off-loaded)	213.95(added)	18.93(off-loaded)
Re-phased-Error	195.44(off-loaded)	214.52(added)	9.71(off-loaded)
$\mathbf{s_a^j}$ (kVA)			
Base-C	1197.48	734.63	990.97
Re-phased-C	974.32	968.85	974.41
Base-V-D	1213.23	774.69	1023.18
Re-phased-V-D	1006.48	1004.04	1002.77
Re-phased-Error	1004.57	998.16	1010.93
$\mathbf{s_{margin}^j}$ (kVA)			
Base-C	-97.48	365.37	109.03
Re-phased-C	125.68	131.15	125.59
Base-V-D	-113.23	325.31	76.82
Re-phased-V-D	95.32	95.96	97.23
Re-phased-Error	95.43	101.84	89.05
$\mathbf{p_{loss}^j}$(kW),$\mathbf{q_{loss}^j}$(kvar)			
Base-C	33.11, 41.30	13.46, 11.08	21.91, 25.671
Re-phased-C	22.77, 25.12	24.02, 22.72	19.072, 24.83
Base-V-D	33.50, 41.91	15.09, 12.37	22.87, 27.36
Re-phased-V-D	23.9, 26.59	25.23, 23.90	20.31, 26.54
Re-phased-Error	23.90, 26.59	25.23, 23.90	20.31, 26.54
C=Constant		V-D= voltage-dependent	

4.4.1 Case 1: Re-phasing using constant-power load model

The resulting phase-wise distribution of loads after re-phasing is depicted in Table 4.4. It is observed that, on the main sub-station, the load among the three phases get balanced after re-phasing. The load flow results for base case system and system after re-phaseing is given in Table 4.5. From Table 4.5, it is observed that the minimum system voltages in each of the phases ($Min(V^a)$, $Min(V^b)$, $Min(V^c)$) is low in base case for phase-a compared to the re-phased case. Thus, after rephasing, the overall system voltage profile has improved along the phases. The maximum voltage unbalance at each bus (δV^{ph}_{max}) in case of base case is quite high as compared to the re-phased case. Thus, after rephasing the phase-wise maximum voltage unbalance, Max(δV^{ph}_{max}), reduces considerably i.e. from 0.027 p.u to 0.006 p.u.

In Table 4.3 when constant load is considered, following observations can be made. When the phase-wise aggregated MVA loads, s^j_d, are compared for *Base-C* and the *Re-phased-C*, it is observed that loads are quite evenly distributed across the phases, for the re-phased case. The maximum unbalance, ($max\{|s^a_d - s^b_d|, |s^b_d - s^c_d|, |s^c_d - s^a_d\}|$), in case of *Base-C* is 429.5 kVA($1146.72 - 717.22$); whereas, for *Re-phased-C* case the same is 8.37 kVA. The maximum unbalance in actual terms (s^j_a) is 462.85 kVA and 5.46 kVA for *Base-C* and *Re-phased-C* cases respectively, suggesting that the unbalance in actual MVA terms are smaller for the re-phased case; thereby, suggesting significant effects of losses in phase-balancing problem. The losses are also distributed among the three-phases.

It can be observed that the real and reactive losses invariably reduce when re-phasing is done. This is true for both types of loads; constant-power as well as voltage-dependent. However, the amounts of loss reduction are different. The reductions in losses are reflected in the reduction in actual MVA intake ($s_a = \sum_{j=a}^{c} s^j_a$); which is reduced from 2923.08 kVA in the *Base-C* configuration to 2917.58 kVA in the *Re-phased-C*case.

Table 4.3 shows that in case of *Base-C* loading, s_{margin} can be calculated as 376.92 kVA (3300 - $\sum_{j=a}^{c} s^j_a$); however, the s^a_{margin} is -97.48 kVA (*phase a* is overloaded); whereas, margins, s^b_{margin}, of 365 kVA and s^c_{margin} of 109 kVA are

available on *phases b* and *c* respectively. In case of *Re-phased-C* configuration, it is observed that overall margin,s_{margin}, of 382.42 kVA is available which is almost equally divided among the three-phases. Thus, by re-phasing a load increase of 125.5 kVA can be further allowed on any or all of the phases.

4.4.2 Case 2: Re-phasing using voltage-dependent load model

The resulting phase-wise distribution of loads after re-phasing is depicted in Table 4.6. It is observed that, on the main sub-station, the load among the three phases get balanced after re-phasing. The load flow results for base case system and system after re-phaseing using voltage-dependent load model is given in Table 4.7. The phase-wise system loading in terms of equivalent specified bus loads, $p_{i0}^{a,sp} + jq_{i0}^{a,sp}$, is also given in Table 5.2 for comparison of optimal re-phasing considering voltage depenedecy and contant loads. From Table 4.7, it is observed that the minimum system voltages in each of the phases ($Min(V^a)$, $Min(V^b)$, $Min(V^c)$) is low in base case for phase-a compared to the re-phased case. Thus, after rephasing, the overall system voltage profile has improved along the phases. The maximum voltage unbalance at each bus ($\delta|V|_{max}^{ph}$) in case of base case is quite high as compared to the re-phased case. Thus, after rephasing the phase-wise maximum voltage unbalance, Max($\delta|V|_{max}^{ph}$), reduces considerably i.e. from 0.024 p.u to 0.0095 p.u.

Considering voltage-dependency of loads, it can be observed that the maximum unbalance in s_d^j in case of *Base-V-D* is 406.48 kVA; whereas, for *Re-phased-V-D* the same is 1.88 kVA. The maximum unbalance in actual terms (s_a^j) is 438.54 kVA for the *Base-V-D* and 3.71 kVA for the *Re-phased-V-D* case. Thus, in case of constant-power load, after re-phasing, the maximum unbalance in s_a^j is lower than the maximum unbalance in s_d^j; whereas, when the voltage-dependency is considered, the opposite phenomenon is observed.

Table 4.4: Re-phasing obtained using constant load model

	Base Load (Constant)			Re-Phased (Constant)			Re-Phased (Voltage Dependent)		
Bus	$p_{i0}^{a,sp} + jq_{i0}^{a,sp}$	$p_{i0}^{b,sp} + jq_{i0}^{b,sp}$	$p_{i0}^{c,sp} + jq_{i0}^{c,sp}$	$p_{i0}^{a,sp} + jq_{i0}^{a,sp}$	$p_{i0}^{b,sp} + jq_{i0}^{b,sp}$	$p_{i0}^{c,sp} + jq_{i0}^{c,sp}$	$p_{i0}^{a,sp} + jq_{i0}^{a,sp}$	$p_{i0}^{b,sp} + jq_{i0}^{b,sp}$	$p_{i0}^{c,sp} + jq_{i0}^{c,sp}$
1	979.19+j689.3	587.06+j441.64	803.71+j579.71	789.21+j571.36	787.22+j564.76	790.91+j569.15	802.86+j606.98	797.54+j609.93	799.2+j605.65
2	0.00 +j0.00	0.00 +j0.00	0.00 +j0.00	0.00 +j0.00	0.00 +j0.00	0.00 +j0.00	0.00 +j0.00	0.00 +j0.00	0.00 +j0.00
3	36.00+j21.60	28.80+j19.20	42.00+j26.40	42.00+j26.40	28.80+j19.20	36.00+j21.60	28.80+j19.20	42.00+j26.40	36.00+j21.60
4	57.60+j43.20	4.80+j3.36	48.00+j30.00	48.00+j30.00	4.80+j3.36	57.60+j43.20	4.80+j3.36	48.00+j30.00	57.60+j43.20
5	43.20+j28.80	28.80+j19.20	36.00+j24.00	43.20+j28.80	28.80+j19.20	36.00+j24.00	43.20+j28.80	28.80+j19.20	36.00+j24.00
6	43.20+j28.80	33.60+j24.00	30.00+j30.00	43.20+j28.80	33.60+j24.00	30.00+j30.00	30.00+j30.00	33.60+j24.00	43.20+j28.80
7	0.00+j0.00	0.00+j0.00	0.00+j0.00	0.00+j0.00	0.00+j0.00	0.00+j0.00	0.00+j0.00	0.00+j0.00	0.00+j0.00
8	43.20+j28.80	28.80+j19.20	3.60+j2.40	43.20+j28.80	28.80+j19.20	3.60+j2.40	43.20+j28.80	28.80+j19.20	3.60+j2.40
9	72.00+j50.40	38.40+j28.80	48.00+j30.00	48.00+j30.00	72.00+j50.40	38.40+j28.80	38.40+j28.80	48.00+j30.00	72.00+j50.40
10	36.00+j21.60	28.80+j19.20	42.00+j26.40	36.00+j21.60	28.80+j19.20	42.00+j26.40	42.00+j26.40	28.80+j19.20	36.00+j21.60
11	50.40+j31.68	24.00+j14.40	36.00+j24.00	36.00+j24.00	24.00+j14.40	50.40+j31.68	24.00+j14.40	36.00+j24.00	50.40+j31.68
12	57.60+j36.00	48.00+j33.60	48.00+j36.00	48.00+j36.00	48.00+j33.60	57.60+j36.00	57.60+j36.00	48.00+j33.60	48.00+j36.00
13	64.80+j21.60	33.60+j21.12	36.00+j24.00	36.00+j24.00	64.80+j21.60	33.60+j21.12	64.80+j21.60	36.00+j24.00	33.60+j21.12
14	57.60+j36.00	38.40+j28.80	60.00+j42.00	57.60+j36.00	38.40+j28.80	60.00+j42.00	38.40+j28.80	60.00+j42.00	57.60+j36.00
15	7.20+j4.32	4.80+j2.88	6.00+j3.60	6.00+j3.60	7.20+j4.32	4.80+j2.88	6.00+j3.60	7.20+j4.32	4.80+j2.88
16	57.60+j4.32	3.84+j28.80	48.00+j36.00	57.60+j4.32	3.84+j28.80	48.00+j36.00	3.84+j28.80	57.60+j4.32	48.00+j36.00
17	57.60+j43.20	33.60+j24.00	54.00+j38.40	33.60+j24.00	57.60+j43.20	54.00+j38.40	33.60+j24.00	57.60+j43.20	54.00+j38.40
18	57.60+j43.20	38.40+j28.80	48.00+j36.00	48.00+j36.00	57.60+j43.20	38.40+j28.80	57.60+j43.20	38.40+j28.80	48.00+j36.00
19	8.64+j6.48	4.80+j3.36	6.00+j4.80	6.00+j4.80	4.80+j3.36	8.64+j6.48	8.64+j6.48	4.80+j3.36	6.00+j4.80
20	50.40+j36.00	38.40+j28.80	54.00+j38.40	50.40+j36.00	54.00+j38.40	38.40+j28.80	54.00+j38.40	38.40+j28.80	50.40+j36.00
21	5.76+j4.32	3.36+j2.40	5.40+j3.84	5.40+j3.84	3.36+j2.40	5.76+j4.32	3.36+j2.40	5.76+j4.32	5.40+j3.84
22	72.00+j50.40	57.60+j43.20	60.00+j48.00	60.00+j48.00	57.60+j43.20	72.00+j50.40	72.00+j50.40	57.60+j43.20	60.00+j48.00
23	8.64+j64.80	4.80+j3.84	60.00+j42.00	8.64+j64.80	60.00+j42.00	4.80+j3.84	60.00+j42.00	8.64+j64.80	4.80+j3.84
24	50.40+j36.00	43.20+j30.72	4.80+j3.60	4.80+j3.60	50.40+j36.00	43.20+j30.72	50.40+j36.00	43.20+j30.72	4.80+j3.60
25	8.64+j6.48	4.80+j2.88	6.00+j4.20	4.80+j2.88	6.00+j4.20	8.64+j6.48	6.00+j4.20	4.80+j2.88	8.64+j6.48
	$p_{ph_d}^{a} + jq_{ph_d}^{a}$	$p_{ph_d}^{b} + jq_{ph_d}^{b}$	$p_{ph_d}^{c} + jq_{ph_d}^{c}$	$p_{ph_d}^{a} + jq_{ph_d}^{a}$	$p_{ph_d}^{b} + jq_{ph_d}^{b}$	$p_{ph_d}^{c} + jq_{ph_d}^{c}$	$p_{ph_d}^{a} + jq_{ph_d}^{a}$	$p_{ph_d}^{b} + jq_{ph_d}^{b}$	$p_{ph_d}^{c} + jq_{ph_d}^{c}$
	951.64+j666.21	586.93+j475.19	789.43+j594.79	778.99+j580.20	772.32+j585.94	778.64+j579.23	775.16+j582.23	772.84+j582.23	782.11+j588.40

Table 4.5: Comparison of voltages after and before Re-phasing for constant load model

	Base Case				After Re-Phasing			
Bus	$V^a(Ang)$	$V^b(Ang)$	$V^c(Ang)$	δV_{max}^{ph}	$V^a(Ang)$	$V^b(Ang)$	$V^c(Ang)$	δV_{max}^{ph}
1	1.050 (0.000)	1.050 (-120.000)	1.050 (120.000)	0.000	1.050 (0.000)	1.050 (-120.000)	1.050 (120.000)	0.000
2	1.026 (-0.587)	1.037 (-120.121)	1.032 (119.593)	0.011	1.031 (-0.375)	1.031 (-120.272)	1.034 (119.551)	0.003
3	1.021 (-0.690)	1.035 (-120.154)	1.028 (119.496)	0.014	1.026 (-0.431)	1.027 (-120.343)	1.031 (119.450)	0.005
4	1.018 (-0.725)	1.034 (-120.167)	1.026 (119.458)	0.016	1.024 (-0.436)	1.025 (-120.376)	1.029 (119.406)	0.005
5	1.017 (-0.730)	1.033 (-120.165)	1.025 (119.456)	0.016	1.023 (-0.441)	1.024 (-120.375)	1.028 (119.404)	0.005
6	1.014 (-0.702)	1.030 (-120.062)	1.022 (119.581)	0.016	1.020 (-0.434)	1.022 (-120.244)	1.024 (119.522)	0.004
7	1.003 (-0.811)	1.024 (-119.999)	1.013 (119.557)	0.021	1.012 (-0.487)	1.013 (-120.212)	1.016 (119.480)	0.004
8	1.012 (-0.710)	1.029 (-120.074)	1.022 (119.589)	0.017	1.018 (-0.442)	1.020 (-120.256)	1.024 (119.529)	0.006
9	0.997 (-0.868)	1.020 (-119.986)	1.008 (119.546)	0.023	1.007 (-0.494)	1.008 (-120.230)	1.011 (119.456)	0.004
10	0.992 (-0.919)	1.017 (-119.977)	1.004 (119.537)	0.025	1.003 (-0.502)	1.004 (-120.245)	1.007 (119.433)	0.004
11	0.990 (-0.946)	1.016 (-119.974)	1.003 (119.536)	0.026	1.002 (-0.503)	1.002 (-120.256)	1.005 (119.422)	0.004
12	0.989 (-0.949)	1.015 (-119.973)	1.002 (119.539)	0.026	1.001 (-0.501)	1.001 (-120.255)	1.004 (119.420)	0.003
13	0.989 (-0.964)	1.015 (-119.974)	1.002 (119.537)	0.027	1.001 (-0.503)	1.001 (-120.273)	1.005 (119.422)	0.004
14	1.000 (-0.824)	1.022 (-119.985)	1.010 (119.550)	0.022	1.010 (-0.492)	1.010 (-120.199)	1.013 (119.468)	0.003
15	1.000 (-0.825)	1.022 (-119.985)	1.010 (119.550)	0.022	1.010 (-0.492)	1.010 (-120.200)	1.013 (119.468)	0.003
16	1.003 (-0.851)	1.024 (-119.961)	1.012 (119.551)	0.021	1.011 (-0.527)	1.013 (-120.174)	1.014 (119.474)	0.003
17	0.999 (-0.821)	1.021 (-119.983)	1.009 (119.553)	0.023	1.009 (-0.489)	1.009 (-120.195)	1.012 (119.468)	0.003
18	1.016 (-0.699)	1.031 (-120.136)	1.024 (119.496)	0.015	1.022 (-0.424)	1.023 (-120.334)	1.027 (119.443)	0.005
19	1.014 (-0.702)	1.030 (-120.129)	1.022 (119.495)	0.016	1.020 (-0.423)	1.021 (-120.333)	1.026 (119.443)	0.006
20	1.014 (-0.702)	1.030 (-120.129)	1.022 (119.494)	0.016	1.020 (-0.424)	1.021 (-120.334)	1.026 (119.443)	0.006
21	1.013 (-0.698)	1.029 (-120.130)	1.021 (119.508)	0.016	1.019 (-0.415)	1.020 (-120.327)	1.024 (119.445)	0.005
22	1.010 (-0.698)	1.027 (-120.124)	1.019 (119.519)	0.017	1.017 (-0.405)	1.018 (-120.321)	1.021 (119.446)	0.005
23	1.016 (-0.686)	1.033 (-120.168)	1.025 (119.459)	0.017	1.023 (-0.383)	1.023 (-120.387)	1.028 (119.402)	0.006
24	1.015 (-0.686)	1.032 (-120.174)	1.025 (119.463)	0.017	1.023 (-0.377)	1.022 (-120.384)	1.027 (119.396)	0.006
25	1.014 (-0.686)	1.032 (-120.175)	1.024 (119.463)	0.017	1.023 (-0.378)	1.021 (-120.383)	1.027 (119.396)	0.006
	$Min(V^a)$	$Min(V^b)$	$Min(V^c)$	Max(δV_{max}^{ph})	$Min(V^a)$	$Min(V^b)$	$Min(V^c)$	Max(δV_{max}^{ph})
	0.989	1.015	1.002	0.027	1.001	1.001	1.004	0.006

Table 4.6: Re-phasing obtained considering voltage-dependency

	Base Load (Voltage Dependant)			Re-Phased (Voltage Dependent)			Re-Phased-Error		
Bus	$p_i^{a,sp}+jq_i^{a,sp}$	$p_i^{b,sp}+jq_i^{b,sp}$	$p_i^{c,sp}+jq_i^{c,sp}$	$p_i^{a,sp}+jq_i^{a,sp}$	$p_i^{b,sp}+jq_i^{b,sp}$	$p_i^{c,sp}+jq_i^{c,sp}$	$p_i^{a,sp}+jq_i^{a,sp}$	$p_i^{b,sp}+jq_i^{b,sp}$	$p_i^{c,sp}+jq_i^{c,sp}$
1	985.14+j708.12	602.03+j487.56	812.30+j622.15	802.86+j606.98	797.54+j609.93	799.20+j605.65	799.06+j608.82	798.08+j599.49	802.42+j614.94
2	0.00+j0.00	0.00+j0.00	0.00+j0.00	0.00+j0.00	0.00+j0.00	0.00+j0.00	0.00+j0.00	0.00+j0.00	0.00+j0.00
3	36.67+j23.41	28.80+j21.92	42.20+j30.90	28.80+j21.18	42.19+j30.79	36.99+j24.32	42.19+j30.58	28.80+j21.31	36.97+j24.27
4	57.78+j47.86	4.94+j3.82	48.21+j34.72	4.90+j3.68	48.20+j34.54	57.89+j51.17	48.19+j34.34	4.91+j3.70	57.88+j50.89
5	44.26+j30.41	30.19+j21.36	37.30+j26.00	44.60+j30.95	29.81+j20.75	37.52+j26.34	44.62+j30.98	29.83+j20.78	37.47+j26.26
6	44.09+j30.15	33.77+j28.43	30.58+j32.64	30.56+j32.52	33.72+j27.03	44.72+j31.14	44.47+j30.74	33.72+j27.14	30.64+j32.94
7	0.00+j0.00	0.00+j0.00	0.00+j0.00	0.00+j0.00	0.00+j0.00	0.00+j0.00	0.00+j0.00	0.00+j0.00	0.00+j0.00
8	43.94+j29.92	30.00+j21.05	3.67+j2.61	44.37+j30.59	29.62+j20.46	3.68+j2.63	44.32+j30.50	29.65+j20.50	3.68+j2.63
9	71.96+j49.47	38.53+j32.13	48.06+j31.30	38.45+j30.12	48.05+j31.16	72.11+j53.05	48.05+j31.14	72.09+j52.44	38.47+j30.51
10	35.74+j20.93	29.47+j20.41	42.02+j26.93	42.03+j26.93	28.92+j19.42	36.16+j22.02	36.08+j21.81	28.92+j19.42	42.04+j27.31
11	50.31+j29.82	24.31+j15.22	36.09+j24.13	24.03+j14.48	36.06+j24.09	50.43+j32.25	36.03+j24.05	24.02+j14.46	50.43+j32.41
12	57.48+j33.67	48.11+j36.30	48.01+j36.14	57.60+j36.07	48.00+j33.64	48.02+j36.44	48.00+j35.94	48.00+j33.63	57.63+j36.60
13	64.14+j20.65	33.68+j22.86	36.05+j24.07	64.82+j21.63	36.03+j24.04	33.61+j21.42	36.00+j24.00	64.80+j21.61	33.62+j21.53
14	57.60+j36.09	38.54+j32.53	60.10+j44.34	38.47+j30.70	60.08+j44.01	57.72+j38.58	57.69+j37.97	38.47+j30.48	60.13+j45.04
15	7.20+j4.33	4.82+j3.25	6.01+j3.80	6.01+j3.84	7.25+j4.46	4.81+j3.09	6.01+j3.79	7.26+j4.49	4.81+j3.09
16	57.82+j4.36	3.92+j31.44	48.77+j37.32	3.88+j30.24	58.47+j4.47	48.95+j37.62	58.51+j4.47	3.88+j30.19	48.96+j37.63
17	57.49+j43.02	34.20+j25.96	54.07+j40.16	33.90+j24.96	58.13+j44.11	54.10+j40.78	33.85+j24.78	58.28+j44.36	54.10+j40.81
18	58.93+j45.47	40.14+j31.83	49.63+j38.80	59.31+j46.15	39.71+j31.06	49.87+j39.23	49.48+j38.55	59.49+j46.46	39.89+j31.38
19	8.66+j7.02	5.01+j3.70	6.02+j5.42	8.67+j7.20	4.95+j3.61	6.03+j5.53	6.02+j5.36	4.95+j3.59	8.68+j7.48
20	51.04+j38.04	40.08+j31.71	55.71+j41.19	55.48+j40.81	39.65+j30.95	51.52+j39.65	51.28+j38.83	55.65+j41.10	39.83+j31.27
21	5.87+j4.50	3.44+j2.68	5.56+j4.10	3.41+j2.57	5.93+j4.62	5.59+j4.15	5.55+j4.08	3.42+j2.59	5.96+j4.66
22	72.12+j53.36	59.81+j47.02	60.19+j53.19	72.18+j54.80	59.16+j45.87	60.22+j54.23	60.17+j52.62	59.09+j45.76	72.25+j56.70
23	8.76+j68.86	4.94+j4.35	60.25+j48.24	60.21+j47.30	8.82+j70.79	4.93+j4.30	8.81+j70.67	60.23+j47.77	4.92+j4.28
24	51.04+j38.06	45.21+j34.03	4.90+j3.95	51.27+j38.81	44.59+j33.00	4.92+j4.03	4.90+j3.92	51.35+j39.07	44.91+j33.52
25	8.75+j6.84	5.02+j3.19	6.02+j4.82	6.02+j4.69	4.95+j3.09	8.86+j7.24	4.96+j3.09	6.02+j4.74	8.84+j7.18
	$p_{ph_d}^a+jq_{ph_d}^a$	$p_{ph_d}^b+jq_{ph_d}^b$	$p_{ph_d}^c+jq_{ph_d}^c$	$p_{ph_d}^a+jq_{ph_d}^a$	$p_{ph_d}^b+jq_{ph_d}^b$	$p_{ph_d}^c+jq_{ph_d}^c$	$p_{ph_d}^a+jq_{ph_d}^a$	$p_{ph_d}^b+jq_{ph_d}^b$	$p_{ph_d}^c+jq_{ph_d}^c$
	951.64+j666.21	586.93+j475.19	789.43+j594.79	778.99+j580.20	772.32+j585.94	778.64+j579.23	775.16+j582.23	772.84+j582.23	782.11+j588.40

Table 4.7: Comparison of voltages after and before Re-phasing for Voltage-dependent load model

	Base Case				After Re-Phasing			
Bus	$V^a(Ang)$	$V^b(Ang)$	$V^c(Ang)$	δV_{max}^{ph}	$V^a(Ang)$	$V^b(Ang)$	$V^c(Ang)$	δV_{max}^{ph}
1	1.050 (0.000)	1.050 (-120.000)	1.050 (120.000)	0.000	1.050 (0.000)	1.050 (-120.000)	1.050 (120.000)	0.000
2	1.026 (-0.577)	1.036 (-120.098)	1.031 (119.600)	0.010	1.030 (-0.363)	1.031 (-120.250)	1.033 (119.559)	0.004
3	1.020 (-0.675)	1.033 (-120.128)	1.027 (119.510)	0.013	1.025 (-0.459)	1.026 (-120.285)	1.030 (119.471)	0.005
4	1.017 (-0.707)	1.033 (-120.140)	1.025 (119.475)	0.015	1.022 (-0.496)	1.024 (-120.292)	1.029 (119.436)	0.006
5	1.016 (-0.711)	1.032 (-120.138)	1.024 (119.474)	0.016	1.021 (-0.500)	1.023 (-120.290)	1.028 (119.435)	0.006
6	1.014 (-0.694)	1.029 (-120.018)	1.021 (119.592)	0.015	1.020 (-0.356)	1.020 (-120.259)	1.023 (119.527)	0.003
7	1.003 (-0.806)	1.022 (-119.937)	1.012 (119.570)	0.019	1.013 (-0.355)	1.011 (-120.268)	1.014 (119.496)	0.003
8	1.011 (-0.700)	1.027 (-120.028)	1.021 (119.600)	0.016	1.018 (-0.361)	1.019 (-120.270)	1.023 (119.536)	0.005
9	0.997 (-0.867)	1.018 (-119.916)	1.007 (119.558)	0.022	1.008 (-0.393)	1.006 (-120.252)	1.009 (119.474)	0.002
10	0.992 (-0.922)	1.015 (-119.901)	1.003 (119.549)	0.023	1.003 (-0.433)	1.003 (-120.241)	1.005 (119.459)	0.002
11	0.990 (-0.951)	1.014 (-119.895)	1.002 (119.547)	0.024	1.001 (-0.454)	1.001 (-120.236)	1.003 (119.452)	0.002
12	0.989 (-0.956)	1.013 (-119.892)	1.001 (119.550)	0.024	1.000 (-0.457)	1.000 (-120.235)	1.002 (119.455)	0.002
13	0.989 (-0.969)	1.013 (-119.894)	1.001 (119.547)	0.024	1.000 (-0.472)	1.001 (-120.236)	1.002 (119.451)	0.002
14	1.000 (-0.819)	1.021 (-119.918)	1.009 (119.566)	0.020	1.011 (-0.344)	1.008 (-120.259)	1.012 (119.482)	0.004
15	1.000 (-0.820)	1.020 (-119.918)	1.009 (119.566)	0.020	1.011 (-0.345)	1.008 (-120.260)	1.012 (119.482)	0.004
16	1.003 (-0.847)	1.022 (-119.897)	1.011 (119.564)	0.020	1.012 (-0.327)	1.010 (-120.302)	1.013 (119.498)	0.003
17	0.999 (-0.816)	1.020 (-119.914)	1.008 (119.571)	0.021	1.010 (-0.341)	1.006 (-120.254)	1.010 (119.485)	0.004
18	1.015 (-0.678)	1.030 (-120.104)	1.022 (119.517)	0.015	1.020 (-0.461)	1.022 (-120.263)	1.026 (119.481)	0.006
19	1.013 (-0.678)	1.029 (-120.095)	1.021 (119.518)	0.015	1.018 (-0.462)	1.021 (-120.255)	1.024 (119.485)	0.006
20	1.014 (-0.679)	1.029 (-120.096)	1.021 (119.516)	0.015	1.018 (-0.463)	1.021 (-120.255)	1.024 (119.483)	0.006
21	1.012 (-0.673)	1.028 (-120.095)	1.020 (119.536)	0.015	1.017 (-0.455)	1.020 (-120.254)	1.023 (119.501)	0.006
22	1.010 (-0.669)	1.025 (-120.086)	1.017 (119.554)	0.016	1.014 (-0.448)	1.018 (-120.246)	1.021 (119.521)	0.007
23	1.015 (-0.664)	1.032 (-120.140)	1.023 (119.481)	0.016	1.020 (-0.492)	1.022 (-120.253)	1.029 (119.437)	0.008
24	1.014 (-0.663)	1.031 (-120.145)	1.023 (119.485)	0.017	1.019 (-0.490)	1.021 (-120.258)	1.028 (119.441)	0.010
25	1.014 (-0.662)	1.030 (-120.145)	1.023 (119.487)	0.017	1.019 (-0.490)	1.021 (-120.258)	1.028 (119.442)	0.009
	$Min(V^a)$	$Min(V^b)$	$Min(V^c)$	Max(δV_{max}^{ph})	$Min(V^a)$	$Min(V^b)$	$Min(V^c)$	Max(δV_{max}^{ph})
	0.9889	1.013	1.0007	0.0244	1.0003	1.0002	1.002	0.0095

It is observed that the s_a increases from 3011.1 kVA in the *Base-V-D* configuration to 3013.24 kVA in the *Re-phased-V-D* case. This phenomena is opposite of constant-power load assumption.This shows that the voltage improvement due to re-phasing as such increases the load demand. The increase in load demand at individual buses may be insignificant; however, for the system as a whole, it reverses the advantage of loss reduction feature of re-phasing. The re-phasing is quite different for the case when voltage-dependency is considered; except for few buses, phase arrangements at all other buses were different for constant loads and voltage-dependent loads.

From Table 4.3, when compared to *Case 1* a similar inference for s_{margin} can be drawn from *Base-V-D* and *Re-phased-V-D* configurations. However, comparing, for base cases, it is worth noting that the s_{margin} (as well as s^j_{margin}) obtained for *Base-C* configuration is higher as compared to voltage-dependent loads *Base-V-D*. The same phenomenon is observed for corresponding cases of re-phasing. Thus, not considering voltage-dependency for a system may suggest more margins whereas actually it is less.

4.4.3 Case 3: Effect of error in load model

In Table 4.6, column *Re-phased-error*, shows the phase-wise load distribution obtained when the re-phasing obtained using constant load model is run considering voltage dependency of loads. The voltages obtained for this cases were slightely different to that obtained for constant power load model given in Table 4.7. In Table 4.3, implications of non-consideration of voltage-dependency of loads is depicted and investigated through *Re-phased-Error* configuration. Table 4.3 depicts the problems that arise when re-phasing obtained considering loads as constant loads (as usually practiced), gets applied to loads which are actually voltage-dependent. It is observed that when the re-phasing obtained using constant-power load model is used for voltage-dependent loads (*Re-phased-Error*), the phase-wise MVA intakes, s^j_a, are quite unbalanced. It is observed, in general, that after re-phasing the phase-wise losses also get distributed evenly. As $p_{loss}(= \sum_{j=a}^{c} p^j_{loss})$, $q_{loss}(= \sum_{j=a}^{c} q^j_{loss})$ are comparable for *Re-phased-V-D* and *Re-*

phased-Error, it may appear that one can use constant-power load model instead of voltage-dependent load model for re-phasing. However, the p_{loss}, q_{loss} were estimated to be 65.85 $kW, 72.68$ $kvar$ for *Re-phased-C* case whereas, in case of *Re-phased-error*, p_{loss}, q_{loss} actually have values as 69.45 $kW, 77.03$ $kvar$. Thus, the losses would not decrease as normally shown using constant-power load model; rather they would increase. This validates the phenomenon observed in actual scenario [16].

A large amount of demand, Δs_d^j, is shifted from $phase-a$ to $phase-b$ showing the effectiveness of proposed method. The amount of demand transfer Δs_d^j for *Re-phased-C* was found to be quite different compared to that of *Re-phased-V-D*. It is also observed that the amount of load transfer in actual sense would be quite different when the constant model based re-phasing is applied to actual case i.e. *Re-phased-Error* case.

As far as s_{margin}^j is concerned it can be observed that there is large difference between *Re-phased-C* and *Re-phased-Error* cases for all the three-phases. It can be observed that when we use the re-phasing obtained using constant-power load model in actual scenario (*Re-phased-Error*) the s_{margin}^j would be quite unbalance when compared to that of *Re-phased-V-D*. Thus, emphasizing use of load model in such operations.

4.4.4 Summary of Results

The summary of results of important quantities (in p.u.) observed during the investigations are depicted in Table 4.8. The table shows minimum bus voltages in each of the phases as V_{min}^a ,V_{min}^b and V_{min}^c for base and re-phased configurations for voltage-dependent as well as for constant-power loads. It is observed that there is improvement in the minimum system voltage when re-phasing is done; this is observed for both the cases, i.e, constant-power load model as well as voltage-dependent loads. However, when re-phasing obtained using constant-power load model is applied to the actual scenario (Table 4.8: *Re-phased-error*), the voltage correction is not as effective as in re-phasing obtained considering voltage-dependency.

Table 4.8: Summary of Results of important quantities

Load model	Constant	Constant	Voltage-Dependent	Voltage-Dependent	Voltage-Dependent
Loading	*Base-C*	*Re-phased-C*	*Re-phased-Error*	*Base-V-D*	*Re-phased-V-D*
V^a_{min}	0.988664	1.000741	0.99972	0.988917	1.000337
V^b_{min}	1.015017	1.000982	1.000062	1.012962	1.000209
V^c_{min}	1.001716	1.004184	1.002746	1.000664	1.002029
$\|I^a\|$	11.40451	9.279252	9.567353	11.55457	9.585557
$\|I^b\|$	6.996496	9.227119	9.506257	7.378032	9.562241
$\|I^c\|$	9.437811	9.280114	9.628127	9.744569	9.550175
$\|I_0\|$	1.280872	0.013096	0.03929	1.255823	0.007544
$\|I_1\|$	9.278884	9.262147	9.567168	9.556509	9.565964
$\|I_2\|$	1.274242	0.026797	0.049282	1.181555	0.026056
$RMSI$	0.194716	0.00322	0.006588	0.180431	0.002836

For constant-power load model, phase currents at the main sub-station ($|I^a|$, $|I^b|$ and $|I^c|$) get balanced. However, when this re-phasing is applied on the actual scenario, following is observed (i) the main substation currents are on the higher side than those computed using constant-power load assumption. (ii) The zero sequence current ($|I_0|$), for the re-phased configuration, is three times more than those estimated using constant-power load assumption. (iii) negative sequence current ($|I_2|$) almost doubles.

The $RMSI$ after re-phasing in case of constant-power load is estimated to reduce by a factor of 60 compared to base case $RMSI$; but when the re-phasing obtained here is deployed for voltage-dependent scenario it would reduce $RMSI$ by a factor of 30. However, when voltage dependency is considered for *Re-phased-V-D*, the $RMSI$ is reduced by 63 times instead of 30 times compared to corresponding base cases.

In case of constant-power load model, re-phasing process can exploit only load re-arrangement, and phase-wise losses to obtain minimum $RMSI$. While in case of voltage-dependent loads the re-phasing process gets higher degree of freedom in form of adjusting loads and voltages such that better $RMSI$ is obtained. Thus, $RMSI$ obtainable in an actual system may be better than that estimated on basis of constant load model.

The above discussion can be summarized as follows. To obtain optimal re-phasing, re-phasing process should be performed considering voltage-dependency of loads.

The system voltages obtained before and after re-phasing are shown in Figure 4.3 and Figure 4.4 respectively. It can be seen from Figure 4.3 and Figure 4.4 that after re-phasing the voltage differences among the phases reduce and also the overall system voltage profile improves.

For the system studied the program was run for 30 times and in 25 cases the program converged to the fitness value of 0.002836. This was due to the stringent condition of stopping criteria used. The time taken for each run ranged from 35-50 minutes on a core-i7 machine. The average fitness value (0.0030), considering the voltage- dependency, was found to be quite close to the best fitness value (0.002836). The worst case fitness was recorded as 0.0047.

4.4.5 Validation and Comparative Studies

The optimal phase arrangement using GA for a 28-bus system is reported in [13]. The present PSO based algorithm is applied to the system of [13] using conductor data reported in ref. [73] for comparison. From Figure 4.5 it can be observed that the phase arrangements obtained by [13] and the proposed method are quite similar when the phase MVA loadings are compared. In Figure 4.6 negative- and zero- sequence currents and %RMSI obtained by using PSO and GA are compared. The zero-sequence current obtained using the proposed method is one-fourth of that obtained in ref. [13]. The negative-sequence current is also lesser. The unbalance factor (%RMSI) obtained by the proposed method is less than half of that calculated for ref. [13].

To further validate the present approach, the proposed method is applied to a sample daily load profile on 28-bus system. The hourly load appearing at the main sub-station and phase currents for the base case are shown in Figure 4.7. The hourly load and the phase currents after re-phasing are shown in Figure 4.8. From Figures 4.7 and 4.8, it is observed that the balance in the phase currents are significant for the re-phased system. The levels of balance in the system for

base case and after re-phasing are depicted more clearly by plotting the sequence currents in Figure 4.9 and Figure 4.10 respectively. It is observed that there is a marked decrease in negative- and zero-sequence currents in the re-phased system (Figure 4.10) when compared to the base case (Figure 4.9). The minimum system phase voltages for the base case and after re-phasing are plotted in Figure 4.11 and Figure 4.12. The effectiveness of phase-balancing in terms of %RMSI for the daily load curve for the base case and the re-phased system is depicted in Figure 4.13. The energy losses for the system reduced from 9.33% to 8.45% which was reduction of 9.43% on relative terms (0.88% in absolute terms).

After validating the results with the results reported in the literature using GA, optimal phase re-phasing using BO has been obtained to evaluate the performance of BO in the phase-balancing problem. From Figure 4.5, it is observed that level of phase balancing obtained using BO are quite similar to that of PSO.

In Figure 4.6, negative- and zero-sequence currents and %RMSI obtained by BO can be compared with the corresponding values obtained using PSO. The negative- and zero-sequence currents and %RMSI, all these are less than that obtained using PSO.

4.5 Conclusion

It has been demonstrated that re-phasing is sensitive to voltage-dependency of loads. It was found that the voltage improvement due to re-phasing increases the load demand. The increase in load demand at individual buses may be insignificant, but for a system as a whole it is significant enough to reverse the advantage of loss reduction conventionally expected due to re-phasing. It was found that the system after re-phasing may suggest more MVA margins at the main substation if appropriate load model is not considered.

PSO algorithm is successfully applied for feeder re-phasing of radial distribution network. The PSO based method was compared with GA based method on a system reported in the literature to establish the effectiveness of the approach. To further validate the effectiveness of the proposed approach a 24 hour load pattern

was taken. It was found that the system could be balanced substantially in terms of phase currents, phase voltages and losses per phase. The energy losses for the system reduced from 9.33% to 8.45% which was reduction of 9.43% on relative terms. It has been shown that BO is giving promising results.

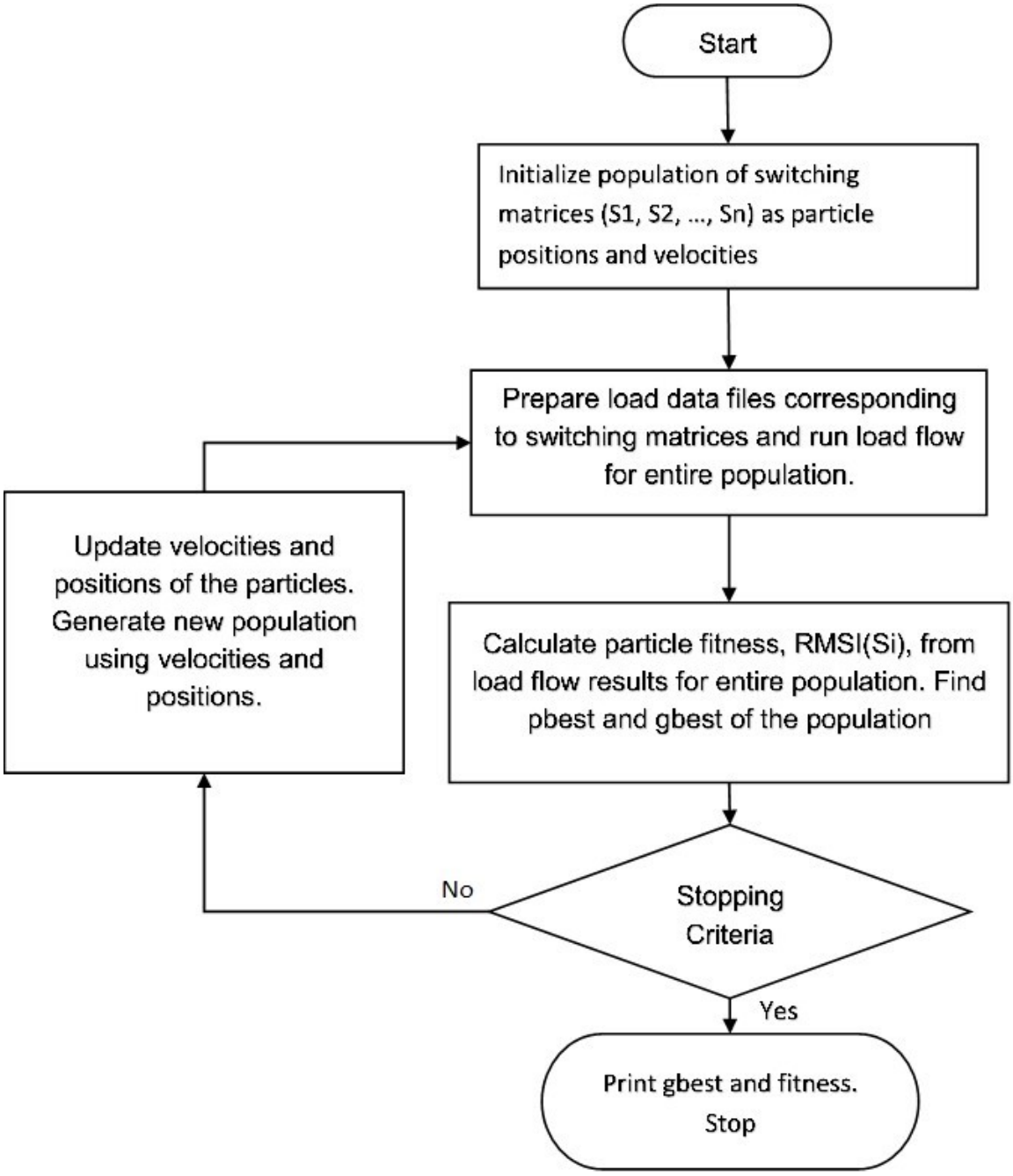

Figure 4.1: Flow chart of re-phasing using PSO.

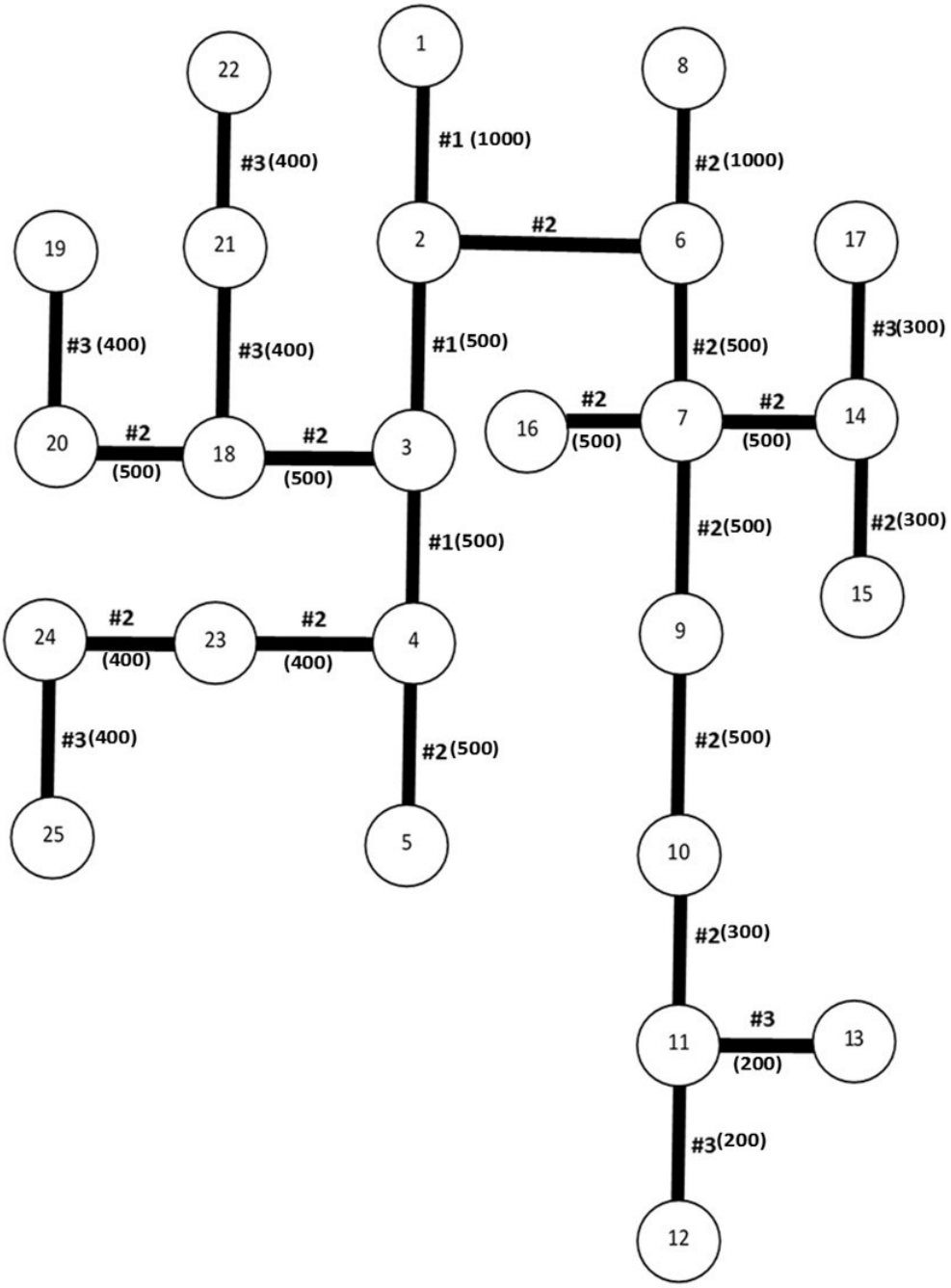

Figure 4.2: Test system showing line type(#) and line length (ft.).

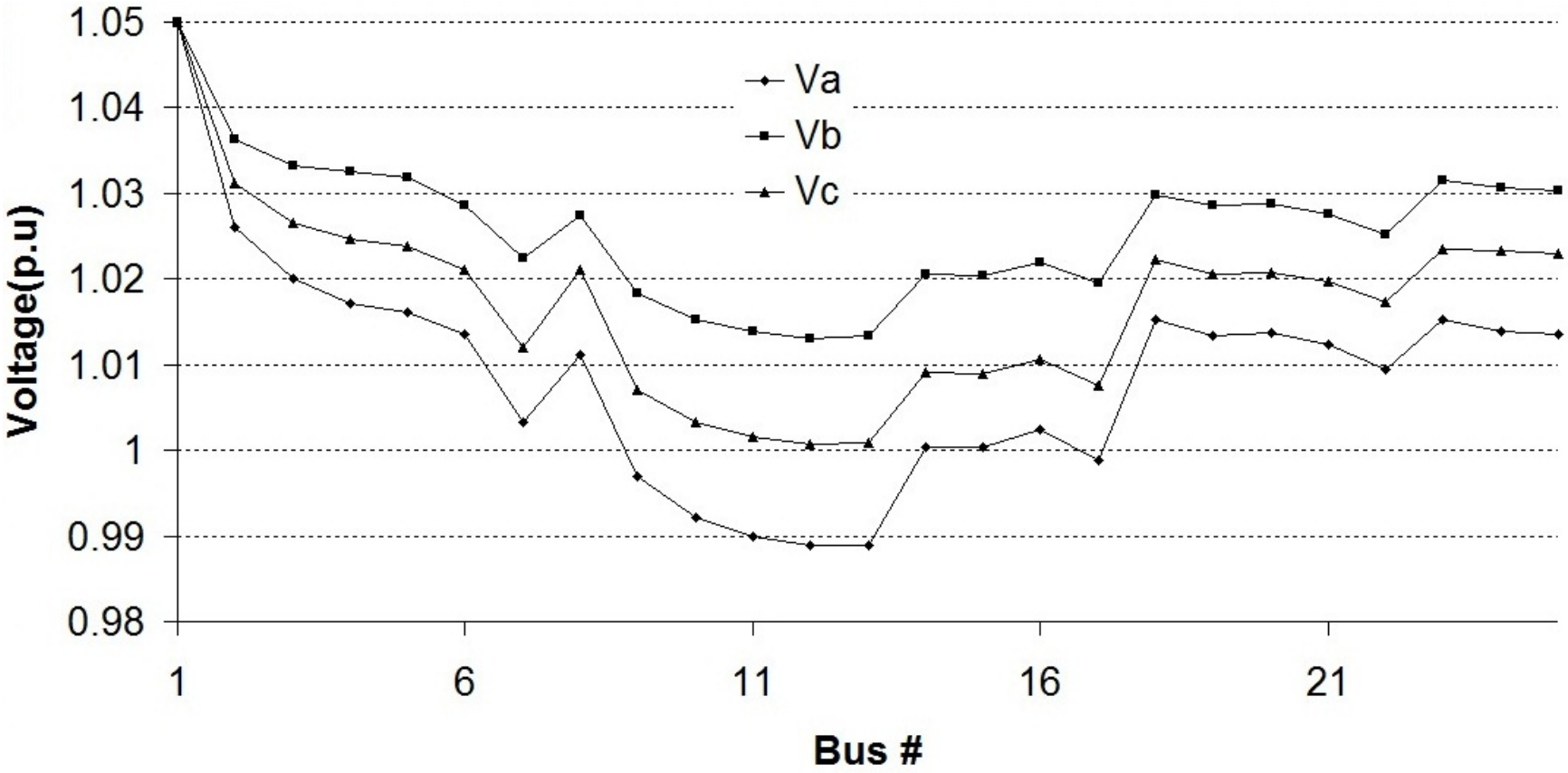

Figure 4.3: System voltages for base case

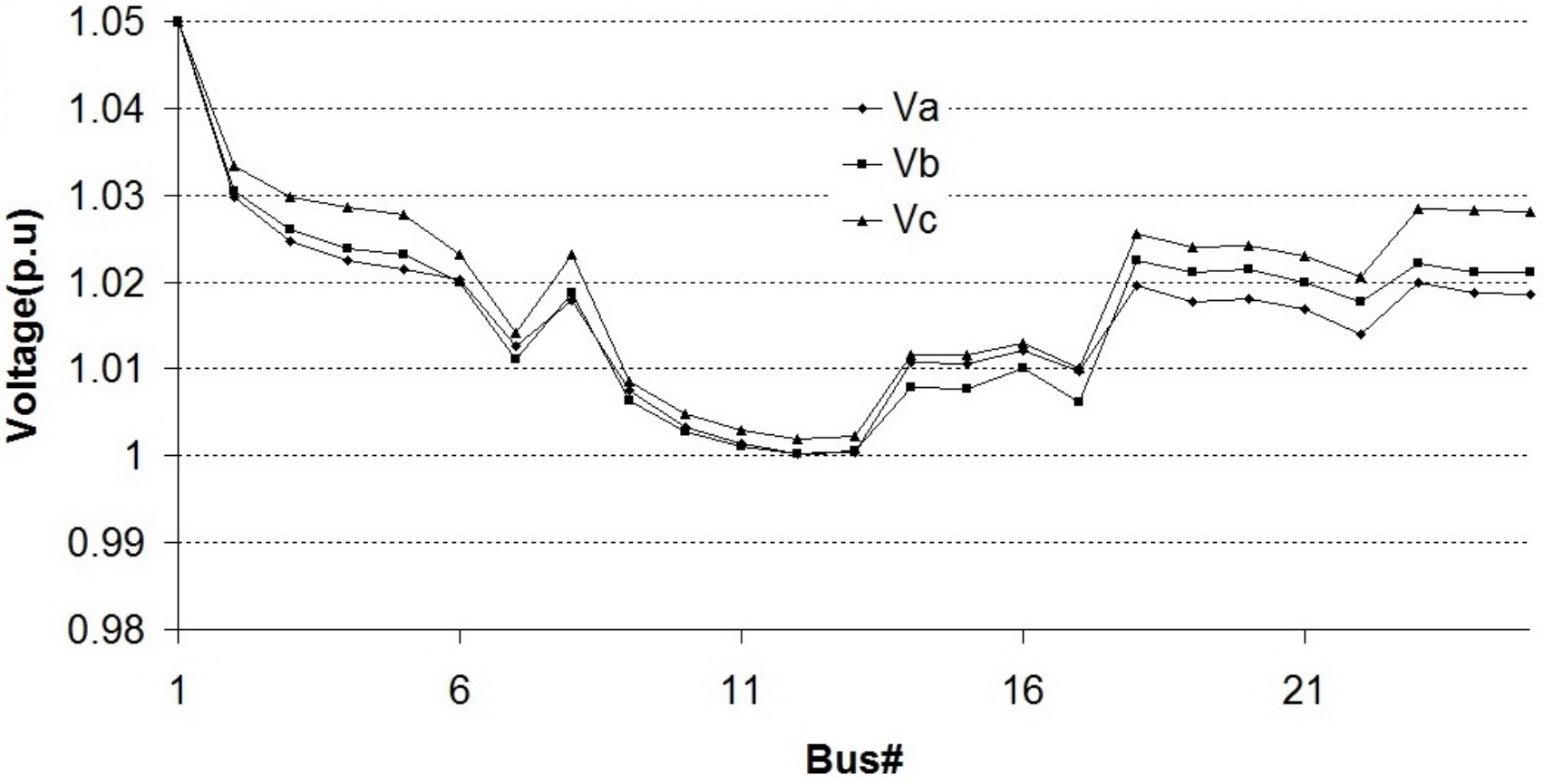

Figure 4.4: System voltages after re-phasing

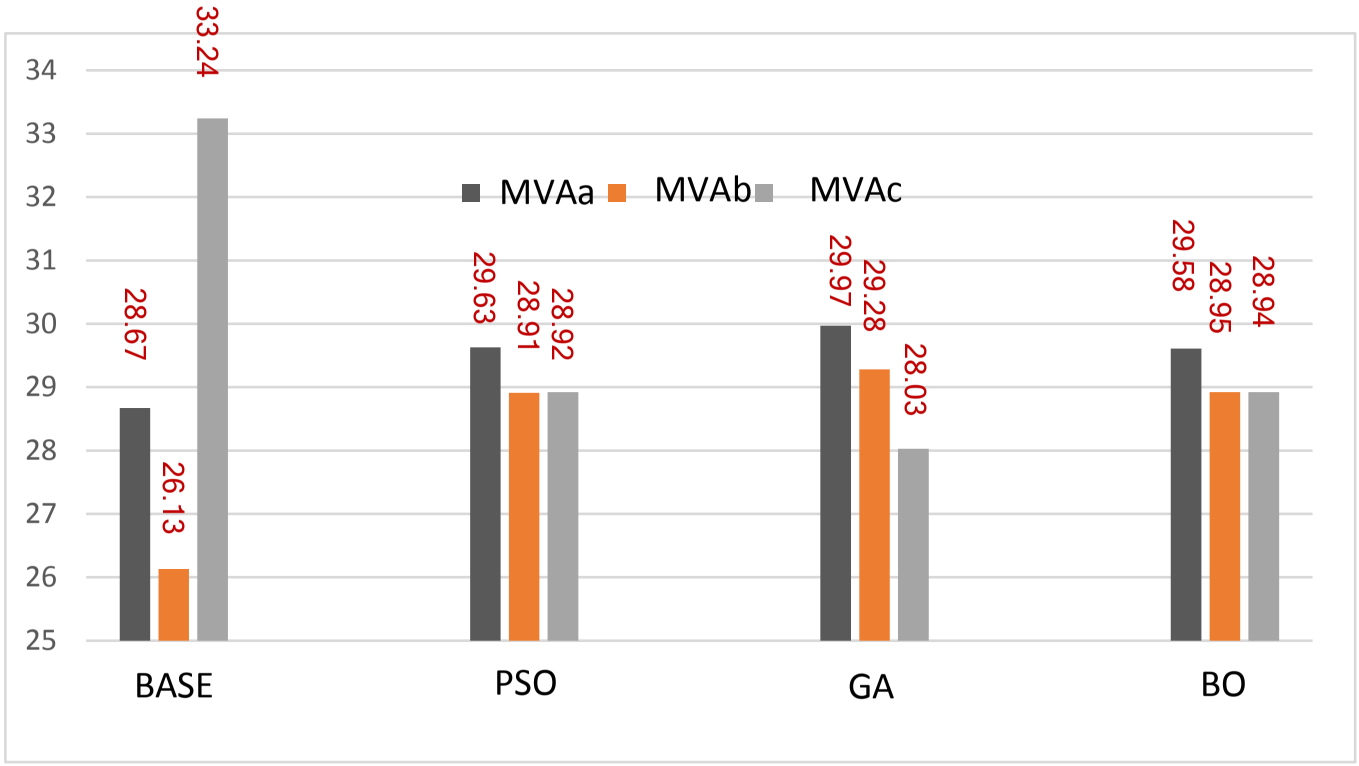

Figure 4.5: Comparison of MVA flows in each phase at the main substation for base case and re-phased case using PSO, GA and BO.

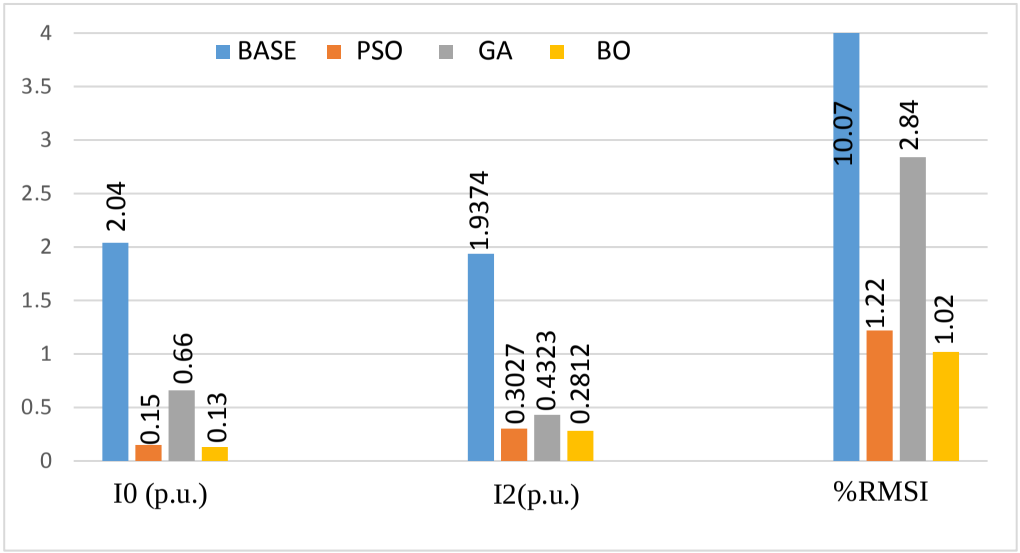

Figure 4.6: Comparison of Sequence Currents and %RMSI for base case and re-phased case using PSO, GA and BO

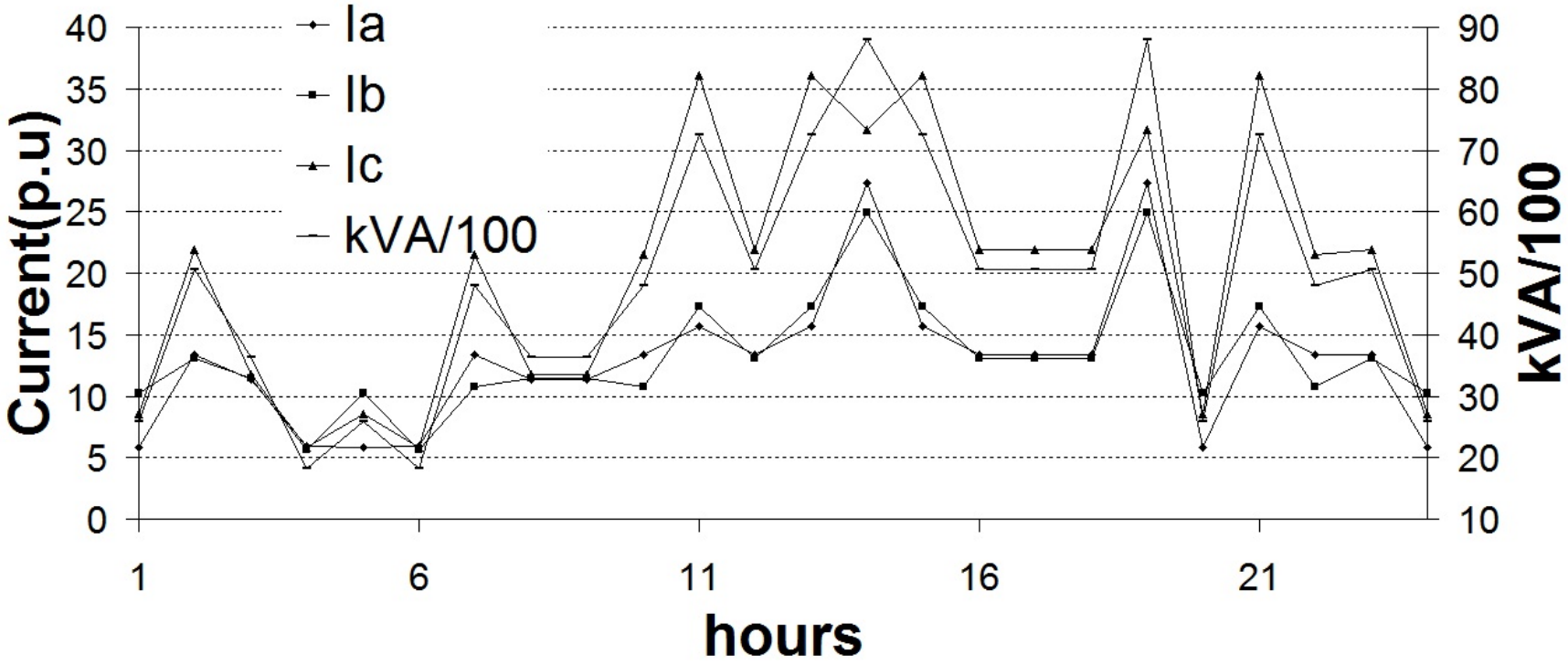

Figure 4.7: Base case phase currents and MVA intake at main sub-station for the system

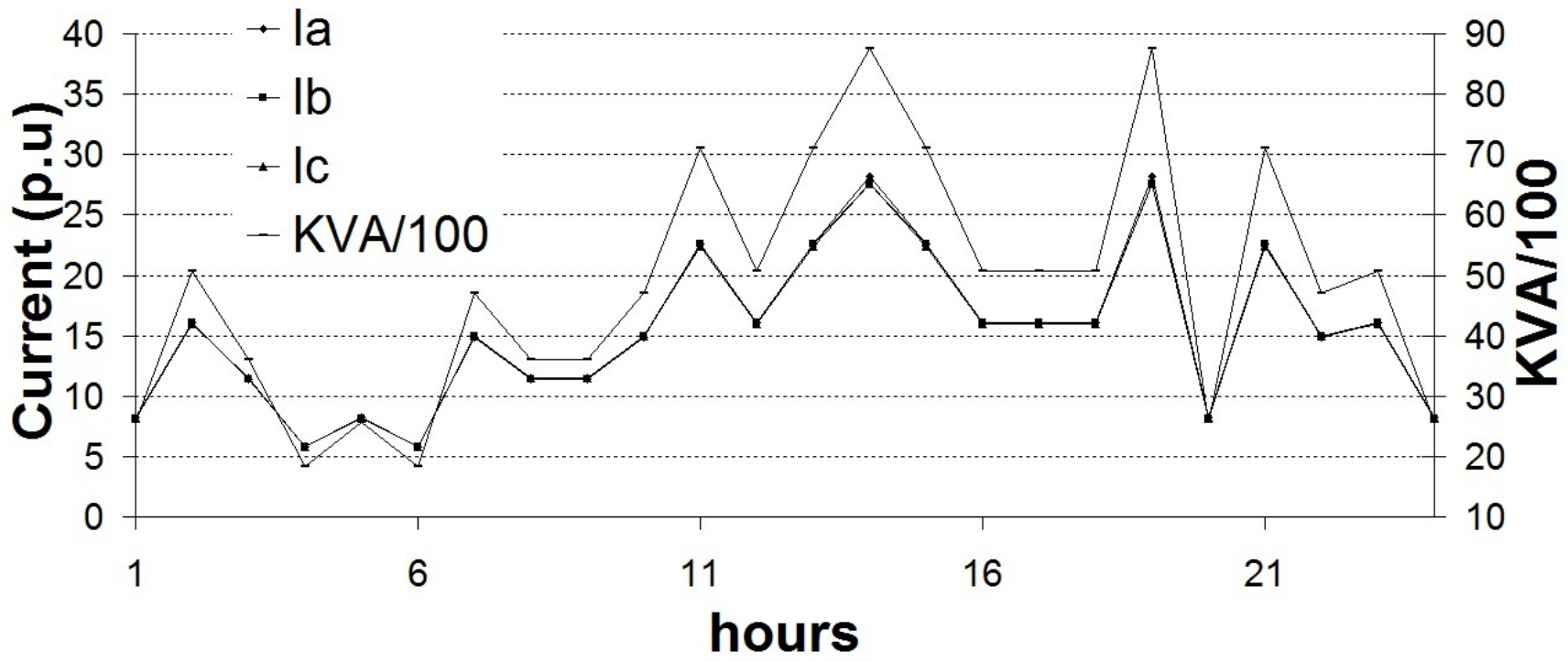

Figure 4.8: Re-phased phase currents and MVA intake at main sub-station.

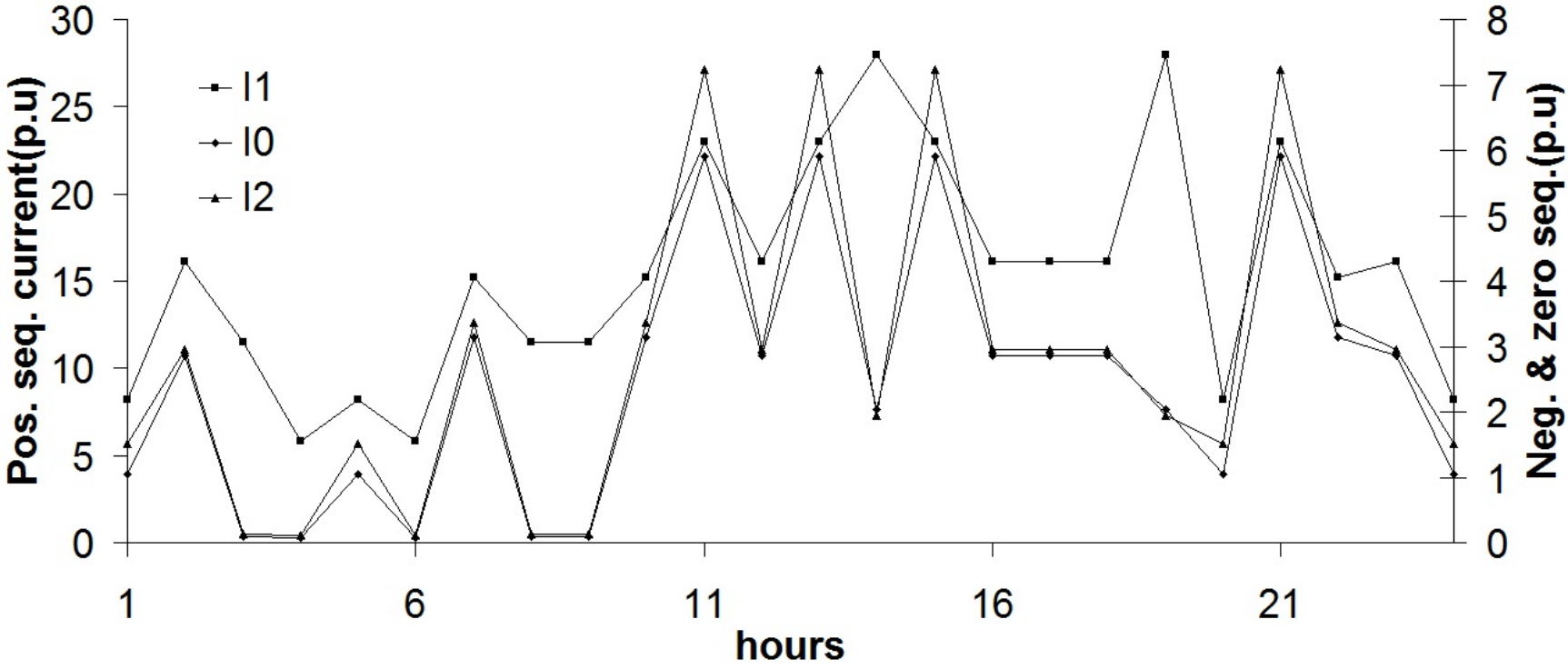

Figure 4.9: Base case sequence currents at main sub-station for the system.

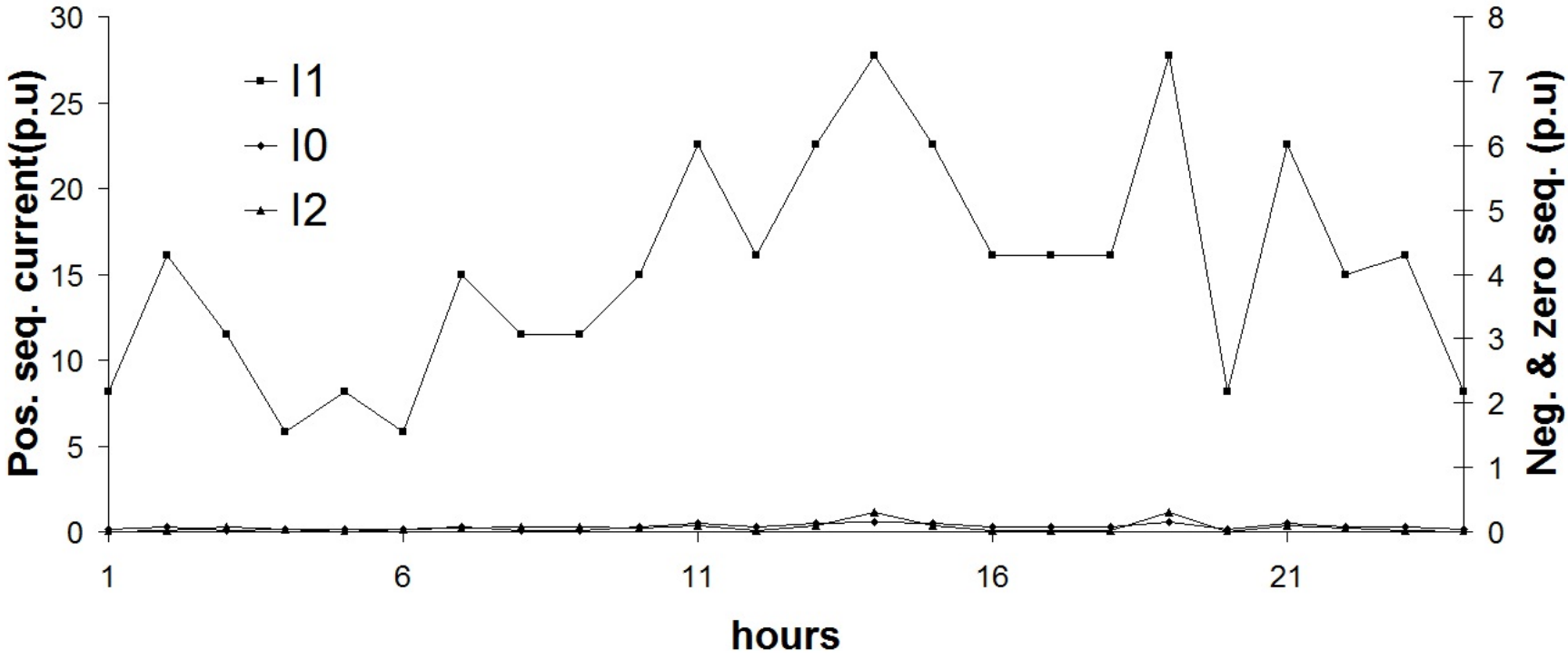

Figure 4.10: Re-phased sequence currents at main sub-station.

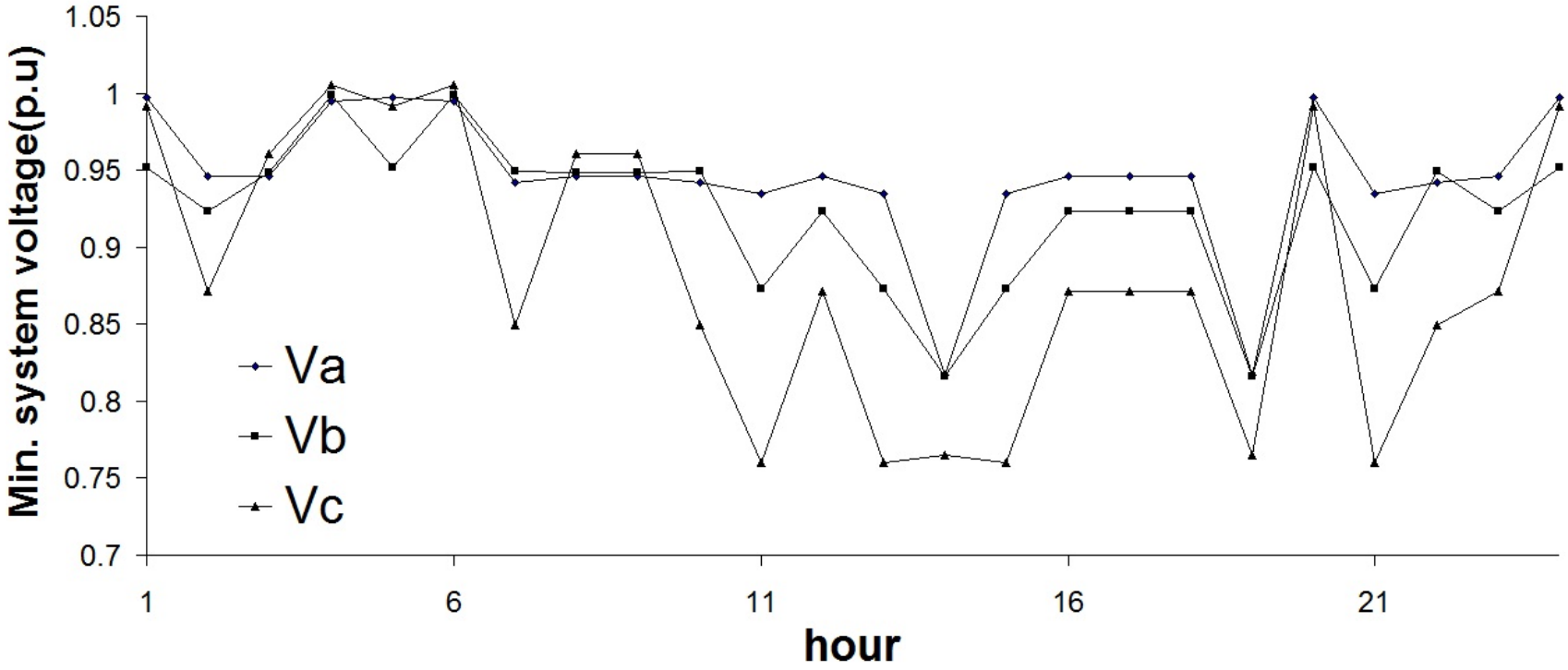

Figure 4.11: Minimum system voltages for the daily load curve for the base case.

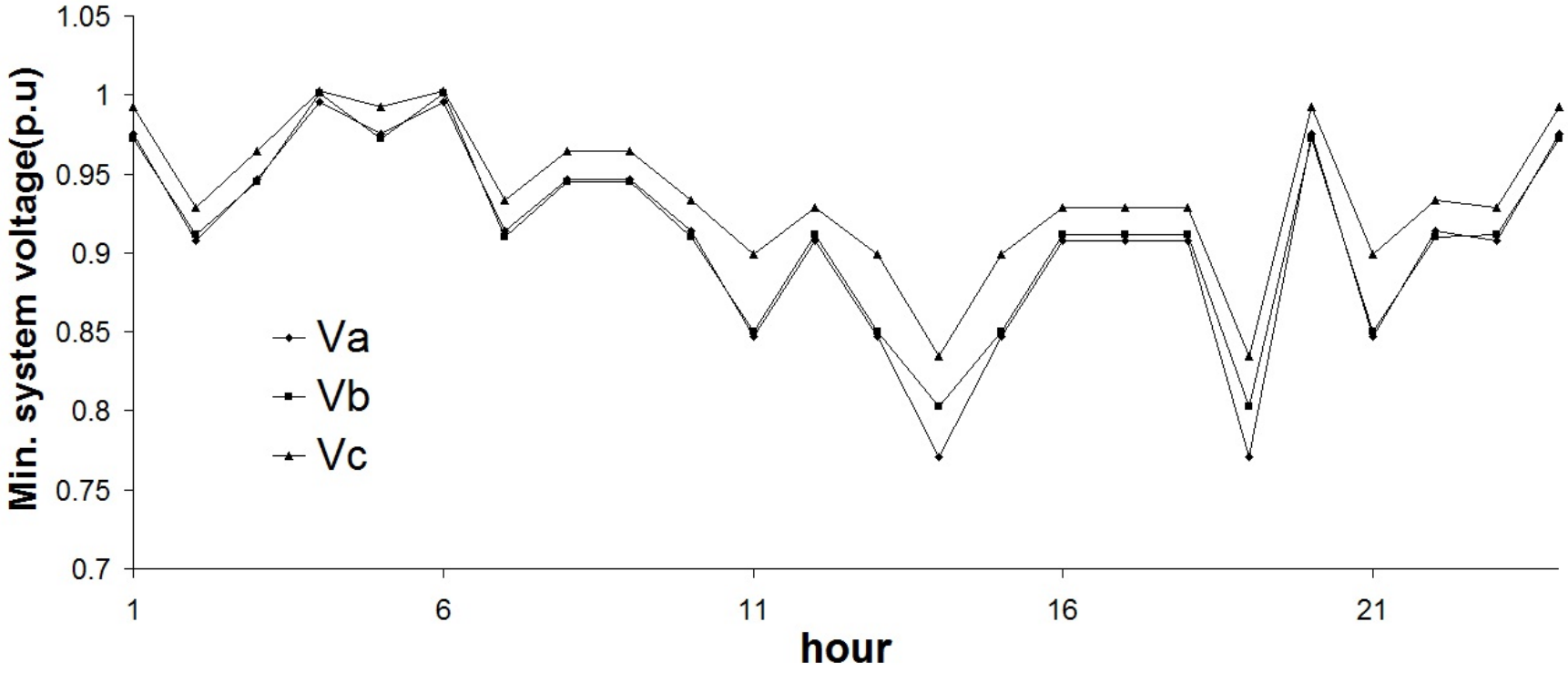

Figure 4.12: Minimum system voltages for the daily load curve for the re-phased system.

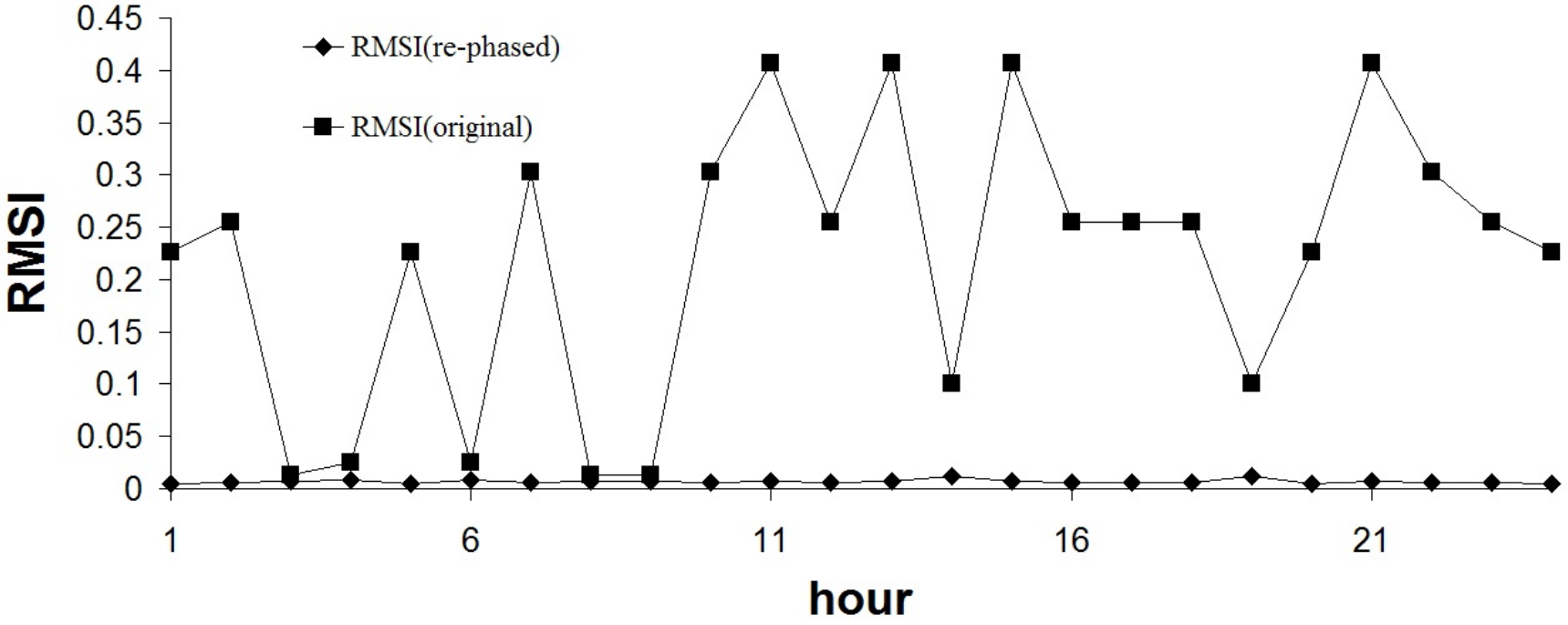

Figure 4.13: RMSI values for base case and re-phased case at main sub-station.